SYNTHESIS AND ELECTROCHROMIC PROPERTIES OF CONDUCTING COPOLYMERS OF DIOXOCINO- AND DITHIOCINO- QUINOXALINES WITH BITHIOPHENE

A THESIS SUBMITTED TO
THE GRADUATE SCHOOL OF NATURAL AND APPLIED SCIENCES
OF
MIDDLE EAST TECHNICAL UNIVERSITY

BY

ŞENİZ BEYAZYILDIRIM

IN PARTIAL FULFILLMENT OF THE REQUIREMENTS
FOR
THE DEGREE OF MASTER OF SCIENCE
IN
CHEMISTRY

JUNE 2005

Approval of the Graduate School of Natural and Applied Sciences.

_____

Prof. Dr. Canan Özgen

Director

I certify that this thesis satisfies all the requirements as a thesis for the degree of Master of Sciences.

_____

Prof. Dr. Hüseyin İşçi

Head of the Department

This is to certify that we have read this thesis and that in our opinion it is fully adequate, in scope and quality, as a thesis for the degree of Master of Sciences.

_____

Prof. Dr. Levent Toppare

Supervisor

Examining Committee Members

Prof. Dr. Duygu Kısakürek	(METU, CHEM)	_____
Prof. Dr. Levent Toppare	(METU, CHEM)	_____
Prof. Dr. Ahmet Önal	(METU, CHEM)	_____
Prof. Dr. Yavuz Ataman	(METU, CHEM)	_____
Prof. Dr. Mustafa Güllü	(Ankara Unv., CHEM)	_____

I hereby declare that all information in this document has been obtained and presented in accordance with academic rules and ethical conduct. I also declare that, as required by these rules and conduct, I have fully cited and referenced all material and results that are not original to this work.

Name, Last name: Şeniz Beyazyıldırım

Signature :

ABSTRACT

SYNTHESIS AND ELECTROCHROMIC PROPERTIES OF CONDUCTING COPOLYMERS OF DIOXOCINO- AND DITHIOCINO- QUINOXALINES WITH BITHIOPHENE

Beyazyıldırım, Şeniz

M.Sc., Department of Chemistry

Supervisor: Prof. Dr. Levent Toppare

June 2005, 59 pages

Two new monomers; 2-benzyl-5,12-dihydro-2*H*-pyrrolo[3',4':2,3][1,4]dioxocino[6,7-b]quinoxaline (DPOQ) and 5,12-dihydrothieno[3',4':2,3][1,4]dithiocino[6,7-b]quinoxaline (DTTQ), were synthesized. The chemical structures of the monomers were characterized by Nuclear Magnetic Resonance (^{1}H-NMR), Fourier Transform Infrared (FTIR) and Mass Spectrometry (MS). Copolymer of DPOQ with bithiophene (BT) was synthesized via potentiostatic electrochemical polymerization in acetonitrile (ACN)-tetrabutylammonium tetrafluoroborate (TBAFB) solvent-electrolyte couple. For DTTQ, copolymerization with bithiophene was achieved via potentiodynamic method in dichloromethane (DCM)-tetrabutylammonium hexafluorophosphate (TBAFP) solvent-electrolyte couple. Characterizations of the resulting copolymers were performed by cyclic voltammetry (CV), FTIR, Scanning Electron Microscopy (SEM) and UV-Vis Spectroscopy. Four-probe technique was used to measure the conductivities of the samples. Moreover, the spectroelectrochemical and electrochromic properties of the copolymer films were investigated. In addition, dual type polymer electrochromic

devices (ECDs) based on P(DPOQ-co-BT) and P(DTTQ-co-BT) with poly(3,4-ethylenedioxythiophene) (PEDOT) were constructed. Spectroelectrochemistry, electrochromic switching and open circuit stability of the devices were studied. They were found to have good switching times, reasonable contrasts and optical memories.

Keywords: Dioxocino- and dithiocino- quinoxaline based monomers; Electrochemical copolymerization; Conducting copolymers; Electrochromism; Spectroelectrochemistry; Electrochromic Devices

ÖZ

DİOKSOSİNO- VE DİTİYOSİNO- KİNOKSALİNLERİN BİTİYOFEN İLE İLETKEN KOPOLİMERLERİNİN SENTEZLENMESİ VE ELEKTROKROMİK ÖZELLİKLERİ

Beyazyıldırım, Şeniz
Yüksek Lisans, Kimya Bölümü
Tez Yöneticisi: Prof. Dr. Levent Toppare

Haziran 2005, 59 sayfa

İki yeni monomer; 2-benzil-5,12-dihidro-2*H*-pirolo[3',4':2,3][1,4]dioksosino[6,7-b]kinoksalin (DPOQ) ve 5,12-dihidrotiyeno[3',4':2,3][1,4]ditiyosino[6,7-b]kinoksalin (DTTQ) sentezlendi. Monomerlerin kimyasal yapıları Nükleer Manyetik Rezonans Spektroskopisi (^{1}H-NMR), Fourier Transform Infrared Spektroskopisi (FTIR) ve Kütle Spektrometri (MS) yöntemleri kullanılarak aydınlatıldı. DPOQ monomerinin bitiyofen (BT) ile kopolimeri, asetonitril (ACN)-tetrabutilamonyum tetrafluoroborat (TBAFB) çözücü-elektrolit sistemi içinde gerçekleştirildi. DTTQ monomerinin bitiyofen ile kopolimeri, diklorometan (DCM)-tetrabutilamonyum heksafluorofosfat (TBAFP) çözücü- destek elektrolit sistemi içersinde gerçekleştirildi. Elde edilen kopolimerlerin karakterizasyonu dönüşümlü voltametri (CV), Taramalı Elektron Mikroskopisi (SEM) ve UV-görünür bölge Spektroskopisi ile gerçekleştirildi. Örneklerin iletkenlikleri dört-nokta tekniği ile belirlendi. Bunların yanı sıra, kopolimerlerin

spektroelektrokimyasal ve elektrokromik özellikleri incelendi. Ek olarak, P(DPOQ-co-BT) ve P(DTTQ-co-BT) kopolimerlerinin poli(3,4-etilendioksitiyofen) (PEDOT) ile elektrokromik cihazları kuruldu. Cihazların spektroelektrokimyasal özellikleri, elektrokromik çevirmeleri ve açık devre hafızaları araştırıldı. Cihazlarin iyi çevirme zamanları, uygun optik kontrastları ve optik hafızaları olduğu bulundu.

Anahtar Kelimeler: Dioksosino- ve ditiyosino- kinoksalin monomerleri; Elektrokimyasal kopolimerizasyon; iletken kopolimerler; Elektrokromizm; Spektroelektrokimya; Elektrokromik Cihazlar

TO MY FAMILY

ACKNOWLEDGMENTS

I express my appreciation to my supervisor Prof. Dr. Levent Toppare for his guidance, support and encouragement during this work.

I would like to express my special thanks to Pınar Çamurlu for her endless helps besides her kind friendship.

I also would like to thank all my lab-mates in our research group for their kind friendship.

Finally I would like to thank my family for always being there for me.

TABLE OF CONTENTS

LIST OF FIGURES

FIGURES

LIST OF TABLES

TABLES

ABBREVIATIONS

ACN	Acetonitrile
BT	2,2'-Bithiophene
CCE	Constant current electrolysis
CIE	The Commission Internationale de l'Eclairge
CP	Conducting polymer
CV	Cyclic voltammetry
DCM	Dichloromethane
DPOQ	2-Benzyl-5,12-dihydro-2*H*-pyrrolo[3',4':2,3][1,4]dioxocino[6,7-b]quinoxaline
DTTQ	5,12-Dihydrothieno[3',4':2,3][1,4]dithiocino[6,7-b]quinoxaline
ECD	Electrochromic device
EDOT	3,4-Ethylenedioxythiophene
FTIR	Fourier transform infrared spectrophotometer
HOMO	Highest occupied molecular orbital
ITO	Tin doped indium oxide
LUMO	Lowest unoccupied molecular orbital
NMR	Nuclear magnetic resonance
PA	Polyacetylene
PBT	Polybithiophene
PC	Propylene carbonate
P(DPOQ-co-BT)	Copolymer of DPOQ and BT
PEDOT	Poly(3,4-ethylenedioxythiophene)
P(DTTQ-co-BT)	Copolymer of DTTQ and BT
PMMA	Poly(methyl methacrylate)
PPy	Polypyrrole
SEM	Scanning electron microscope

TBAFB	Tetrabutylammonium tetrafluoroborate
TBAFP	Tetrabutylammonium hexafluorophosphate

CHAPTER I

INTRODUCTION

1.1. Conducting Polymers

An organic polymer that exhibit highly reversible redox behavior and combination of properties of metals and plastics, is termed as conducting polymer (CP), more commonly, "synthetic metal" [1].

Electron delocalization is a consequence of the presence of conjugated double bonds in the polymer backbone. Figure 1.1 shows the structures of some conducting polymers and to make them electrically conductive, it is necessary to introduce mobile carriers into double bonds, which is achieved by oxidation or reduction reactions (called "doping") [2].

CPs have been investigated extensively since the discovery of conductivity in polyacetylene with an order of 10^{-5} S/cm by Hatano and coworkers [3]. The high levels of conductiviy in polymers was first observed in 1977 when Shirakawa, MacDiarmid and Heeger discovered that oxidation with halogen vapor made polyacetylene films 10^{9} times more conductive than they were originally [4].

Shirakawa, MacDiarmid and Heeger were awarded the Nobel Prize in Chemistry in 2000 "for the discovery and development of electrically conductive polymers". Their remarkable discovery stimulated the world wide efforts to develop new classes of CPs with properties similar to or better than those of polyacetylene [5]. An important step in the development of conjugated poly(heterocycles) occurred in 1979 when Diaz and coworkers obtained polypyrrole (PPy) as a freestanding film

by oxidative electropolymerization of pyrrole [6]. Since this discovery, other aromatic compounds such as aniline [7] and thiophene [8] have been polymerized electrochemically.

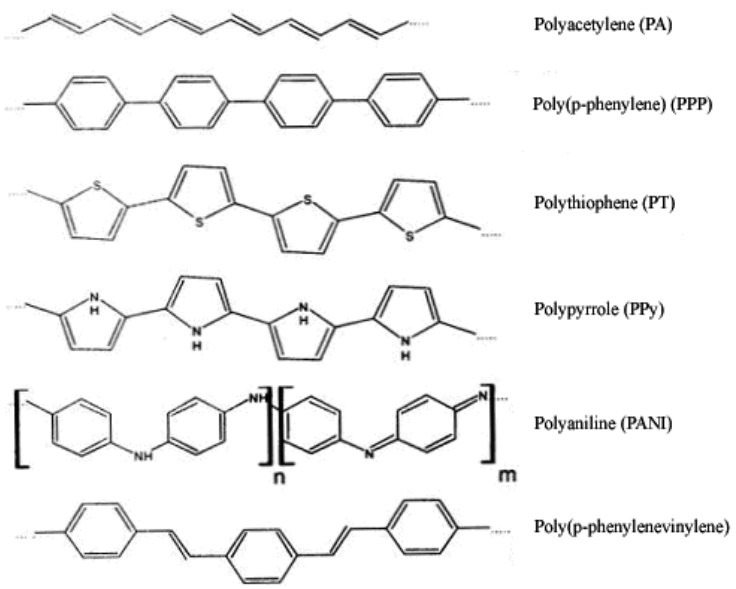

Figure 1.1 Chemical structures of some conducting polymers

Conducting polymers have some disadvantages such as they are insoluble and they possess poor mechanical and physical properties, which restrict their processability. Synthesis of substituted derivatives, composites, graft and block copolymers were shown to be effective to overcome these problems [9-11]. Since the recent developments, conducting polymers having good environmental stability and long term stability of electrical conductivity replace metals and semiconductors in electrical and electronics industry.

At present, conducting polymers are used in wide range of areas such as electrochromic windows or multichromic displays [12], light emitting diodes [13,14], batteries [15,16], gas separation membranes [17] and optical displays [18,19].

1.2 Band Theory

Band theory is widely used to understand the electrical conduction. When two identical atoms each having a half-filled orbital are brought together, the two orbitals interact to produce two new orbitals, one of lower energy and one of higher energy. The magnitude of this energy difference is determined by the extent of orbital overlap. The two electrons go into the lower-energy orbital. The (now-filled) lower-energy orbital is a bonding orbital and the higher-energy (empty) orbital is an antibonding orbital. There is an energy spacing between the highest of the low energy orbitals (HOMOs) and the lowest of the high-energy orbitals (LUMOs) and this is called the band gap (E_g). In other words, E_g is the energy difference between the valence and conduction bands.

In a metal there is no gap. This means that orbitals are freely available for conduction. On the other hand, insulators have a very large band gap, and hence thermal excitation of carriers is not possible. In a semiconductor the magnitude of the gap is such that electrons may be thermally excited across it, putting the electrons into the empty upper band, where they can conduct, and leaving holes in the lower band, which can also conduct [20]. In the case of highly conjugated conducting polymers, the difference between energy levels within these two sets of orbitals is so small that the bands may be regarded as continuous and the electron can take any energy within. Schematic representations of band structures are given in figure 1.2.

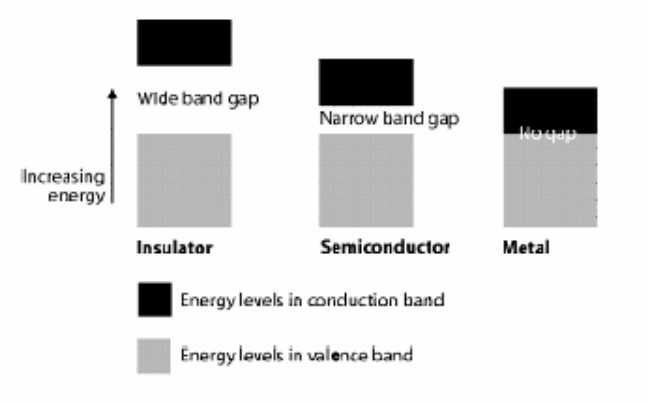

Figure 1.2 Schematic representations of band structures

Electrical conductivity (σ) is proportional to the number of charge carriers (n), the charge (q) and the mobility (μ) on the carriers.

$$\sigma = q\, n\, \mu$$

In semiconductors and electrolyte solutions, one must also add an extra term due to positive charge carriers (holes or cations). Conductivity range is given in figure 1.3.

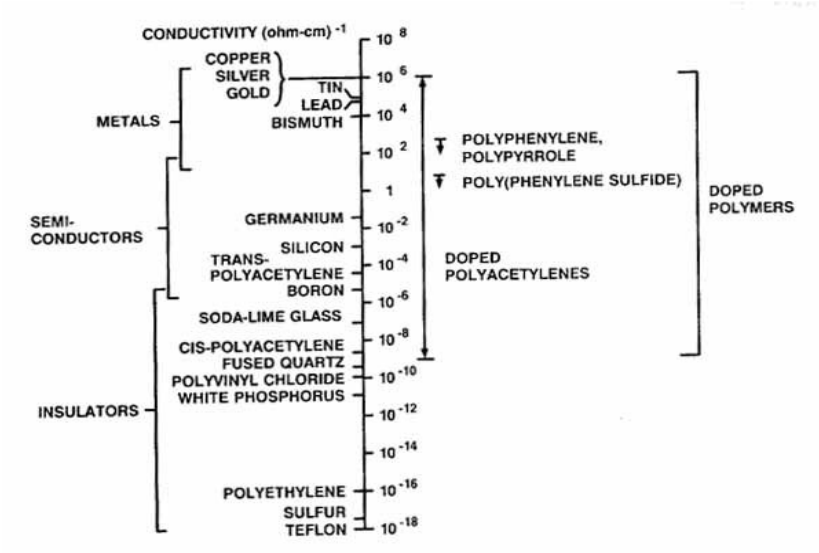

Figure 1.3 Conductivity range

1.3 Doping Process

The properties like structure, surface morphology, electrical conductivity and air stability of the polymers depend upon the nature and extent of doping. Charge injection onto conjugated, semiconducting macromolecular chains, ‘‘doping’’, can be accomplished in a number of ways.

Chemical doping involves charge-transfer redox chemistry:

(a) Oxidation (*p*-type doping)

$(\pi\text{-polymer})_n + 3/2\ ny\ (I_2) \rightarrow [(\pi\text{-polymer})^{+y}\ (I_3^-)_y]_n$ [3];

(b) Reduction (*n*-type doping)

$(\pi\text{-polymer})_n + [Na^+\ (Napthtalide)^*]_y \rightarrow [(Na^+)_y\ (\pi\text{-polymer})^{-y}]_n + (Naphth)^0$ [21].

When the doping level is sufficiently high, the electronic structure evolves to that of metal.

Although chemical doping is an efficient and straightforward process, it is typically difficult to control. Attempts to obtain intermediate doping levels often results in inhomogeneous doping. Electrochemical doping was invented to solve this problem [22]. In electrochemical doping, the electrode supplies the redox charge to the conducting polymer, while ions diffuse into (or out of) the polymer structure from the nearby electrolyte to compensate the electronic charge. The doping level is determined by the voltage between the conducting polymer and the counter electrode; at electrochemical equilibrium the doping level is precisely defined by that voltage. Thus, doping at any level can be achieved by setting the electrochemical cell at a fixed applied voltage and simply waiting for the system to come to electrochemical equilibrium.

Electrochemical doping is illustrated by the following examples:

(a) *p* type

$(\pi\text{-polymer})_n + [Li^+\ (BF_4^-)]_{sol'n} \rightarrow [(\pi\text{-polymer})^{+y}\ (BF_4^-)_y]_n + Li\ (electrode)$;

(b) *n* type

$(\pi\text{-polymer})_n + [Li\ (electrode)] \rightarrow [(Li^+)_y\ (\pi\text{-polymer})^{-y}]_n + [Li^+\ (BF_4^-)]_{sol'n}$ [23].

Increased doping level leads to increased conductivity, via creation of more mobile charges [20].

1.4 Hopping Process

Carrier mobility is the main reason of electrical transport in conducting polymers. Mobility of the charge carriers can be restricted as the degree of overlapping decreases in molecular or atomic levels. As the electronic states become increasingly localized, transport of the particle occurs through hopping process. In order to obtain hopping conduction, it is necessary to have an insulating or semiconducting material exhibiting a few intrinsic thermal free carriers at least over a limited energy region, a large density of sites through which charge transfer can take place. There are mainly three types of transport for the carrier mobility; single chain or intramolecular transport, interchain transport and interparticle contact [24]. The intrachain movement depends on the effective conjugation of the polymer, while the interchain jumping is determined by the stacking of the polymer molecules.

1.5 Solitons, Polarons and Bipolarons

Polymer doping leads to the formation of conjugational defects; solitons, polarons and bipolarons in the polymer chain. The presence of localized electronic states of energies less than the band-gap arising from changes in local bond order, including the formation of solitons, polarons and bipolarons have led to the possibility of new types of charge conduction [1]. Solitons are subdivided into three catogories: neutral soliton, positive soliton and negative soliton. An interesting observation at this point that charged solitons have no spin; however, neutral solitons have spin but no charge. Positively charged soliton occurs when an electron is removed from localised state of a neutral soliton by oxidation. Negatively charged soliton is produced when an electron is inserted by reduction (Figure 1.4).

Polarons are obtained as a combination of a neutral and a charged soliton on the same polymer chain. Further oxidation causes more and more polarons to form

and eventually the unpaired electron of the polaron is removed, or two lose polarons can combine to form dications or bipolarons (Figure 1.5) [25, 26].

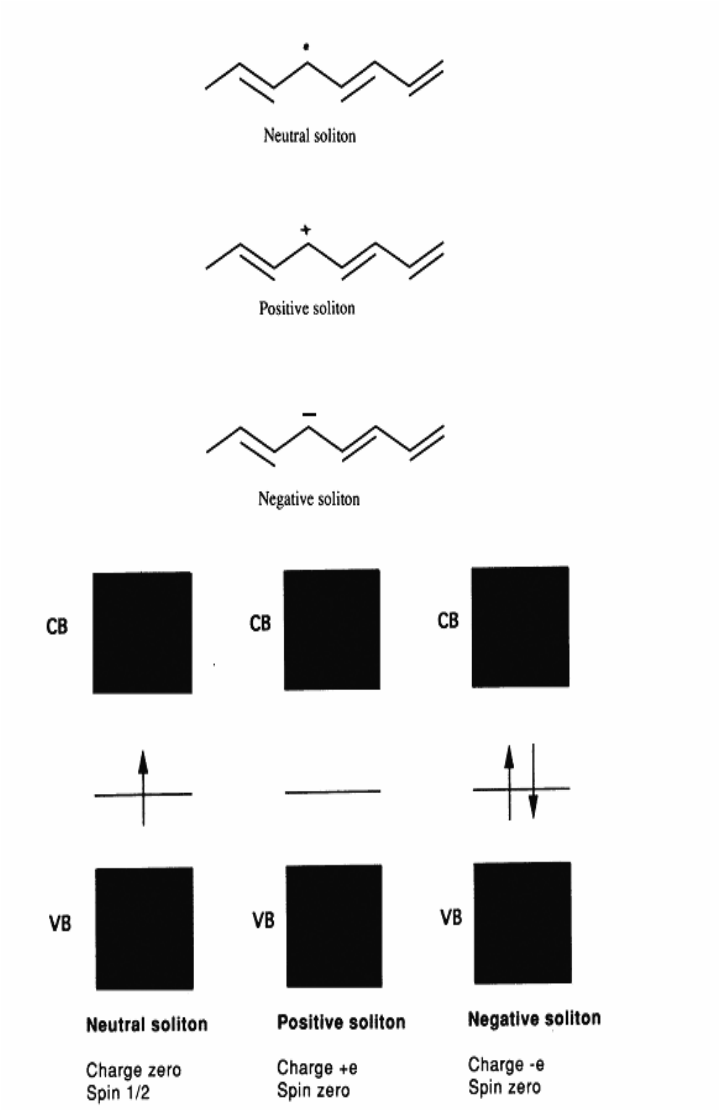

Figure 1.4 Soliton structures of polyacetylene

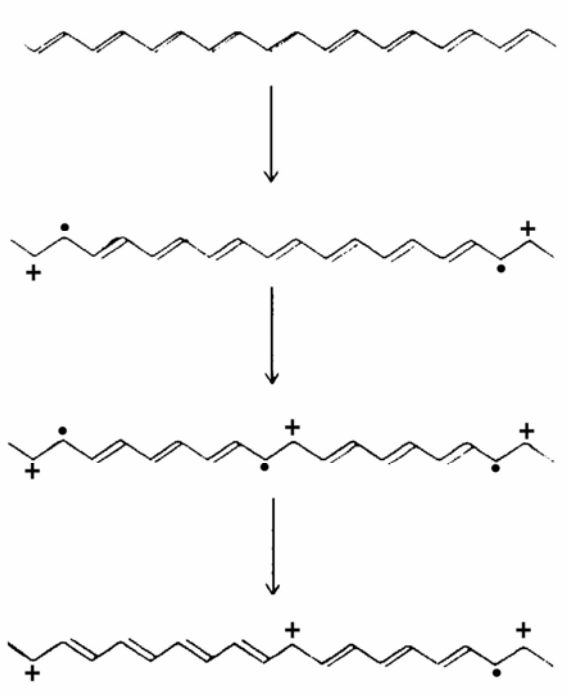

Figure 1.5 Formation of polaron and bipolaron for polyacetylene

The neutral polymer has full valance and empty conduction bands with a separated band gap. Formation of polaron and bipolaron generates new energy levels located at midgap (Figure 1.6).

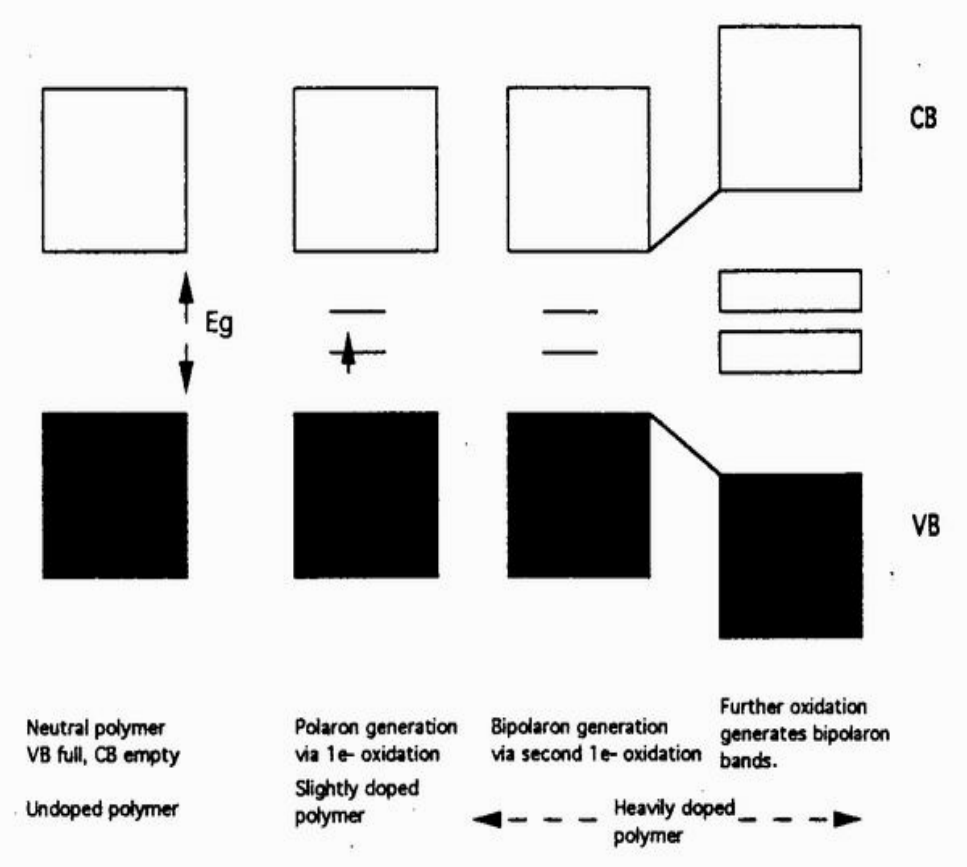

Figure 1.6 Band structure of a conjugated polymer as a function of doping level illustrating polaronic and bipolaronic states in the band gap

1.6 Synthesis of Conducting Polymers by Electrochemical Polymerization

Electrochemical formation of conducting polymers is an unique process. Although it presents some similarities with the electrodeposition of metals since it proceeds via a nucleation and phase-growth mechanism, the major difference lies in the fact that the charged species precursors of the deposited material must be initially produced by oxidation of the neutral monomer at the anode surface [27]. There are many advantages of synthesizing conducting polymers electrochemically [28]:

i) Simple
ii) Selective
iii) Reproducible
iv) Reactions are done at room temperature
v) Thickness of the films can be controlled by varying either the potential or current with time
vi) Homogeneous films can be obtained
vii) Doping of the polymer can be achieved with the desired ion simultaneously
viii) Polymer films are directly formed at the electrode surface
xi) Graft and block copolymers can easily be obtained

Figure 1.7 represents the mechanism proposed for the electropolymerization of heterocycles, by analogy to the already known coupling reactions of aromatic compounds. First elecrochemical step (E) consists the oxidation of the monomer to its radical cation. Since the electron transfer reaction is much faster than the diffusion of the monomer from the bulk solution, it follows that a high concentration of radicals is continuously maintained near the electrode surface. The second step involves the coupling of two radicals to produce a dihydro dimer dication which leads to a dimer after loss of two protons and rearomatization. This rearomatization constitutes the driving force for the chemical step (C). Due to the applied potential, the dimer, which is more easily oxidized than the monomer, occurs in its radical form and undergoes a further coupling with a monomeric radical. Electropolymerization proceeds then through successive electrochemical and chemical steps according to a general $E(CE)_n$ scheme, until the oligomer becomes insoluble in the electrolytic medium and precipitates onto the electrode surface [27].

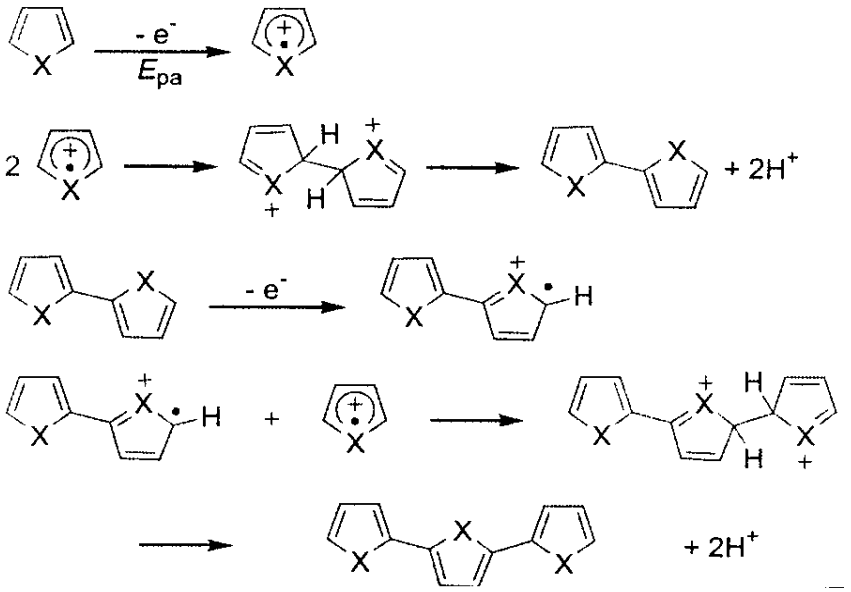

Figure 1.7 Electrochemical polymerization mechanism of five-membered heterocycles

1.7 Electrochemical techniques

1.7.1 Constant Current Electrolysis (Galvanostatic)

In constant current electrolysis (CCE), the current is kept constant throughout the electrolysis while the potential is allowed to alter in a cell containing working and counter electrodes. It is simple in application but it has some disadvantages. The variation of the potential may cause all possible redox process and the nature of the generated species may be unknown because of the side reactions. In order to overcome these difficulties, electrolyte or substrate can be added at the same rate as that of monomer consumption.

1.7.2 Constant Potential Electrolysis (Potentiostatic)

This method is carried out in a three electrode cell, which ensures effective potential control and maximize the reproducibility of the polymerization process. The potential of the working electrode with respect to a reference electrode is adjusted to a desired value and kept constant by a potentiostat. This potential may be called the polymerization potential (E_{pot}) and it is determined by means of cyclic voltammetry. Since the potential is constant during the electrolysis, unwanted electroactive species are eliminated and the initiation proceeds only through monomer.

1.7.3 Cyclic Voltammetry

Cyclic voltammetry is one of the most useful methods, which provides a great deal of useful information about the electrochemical behavior of electroactive species. In this method, the potential of the working electrode is scanned in the anodic and cathodic directions and the current flow as a function of this potential is measured. A voltammogram provides us to understand the electroactivity and redox potential of a material, mechanism of the electrochemical reactions, reversibility of electron transfer, whether the reaction products are further reduced or oxidized and the growth rate of the conducting polymers.

1.8 Effect of Synthesis Conditions on Electrochemical Polymerization

The nature of the process occurring and final properties of the electrogenerated polymers are affected by many parameters such as the nature and shape of the electrodes, solvent, electrolyte, temperature, synthesis potential, cell geometry and monomer concentration.

Since the polymerization proceeds via oxidation and reduction reactions, it is necessary that the electrode should not be oxidized concurrently with the aromatic monomer [29]. For this reason, inert electrodes, such as Pt, Au and ITO are mostly

used when preparing conductive films. Saturated calomel electrode (SCE), Ag/Ag^{+1} and Ag/AgCl electrodes can be used as the reference electrode [30].

Solvent should be capable of dissolving monomer and counterion at appropriate concentrations. In addition, it should present a high dielectric constant to ensure the ionic conductivity of the electrolytic medium and a good electrochemical resistance against decomposition at potentials required to oxidize the monomer. The solvents with poor nucleophilic character should be used since more nucleophilic solvents are likely to attack the free radical intermediates. Therefore, aprotic solvents such as acetonitrile may be used during electropolymerization [6].

The requirements in selecting the supporting electrolyte are basically; the solubility of the salt, its degree of dissociation and the reactivity of both the anion and the cation [30]. In addition to these, the counterion should be stable both chemically and electrochemically; otherwise, breakdown products can interfere in the polymerization process [31].

Temperature is the other parameter that should be taken into consideration during electropolymerization. It has a substantial influence on the kinetics of polymerization as well as on the conductivity, redox properties and mechanical characteristics of the films [32]. At high temperatures, lower conducting films are produced as a result of the side reactions such as solvent discharge and nucleophilic attacks on polymeric radicals [33] .

1.9 Electrochromism

Electrochromism is the reversible change in optical properties that can occur when a material is electrochemically oxidized or reduced. Materials can be considered as being electrochromic when they display distinct visible color changes, with the color change commonly being between a transparent and a colored state, or between two colored states. In cases where more than two redox states are

electrochemically available, the electrochromic material may exhibit several colors and be described as polyelectrochromic [34].

In conducting polymers, the electrochromism, as well the electronic conductivity, is explained using the Band Model: the doping process modifies their electronic structure, producing new electronic states in the band gap and causing the color changes. Electronic absorption shifts to higher wavelengths with doping, and the color contrast between doped and undoped forms is related to the polymer band gap energy, E_g. Simultaneous to doping-undoping process, a mass transport takes place into the polymer bulk due to the counter-ion motion inside the films. The slower process controls the color variation kinetics in polymer films [4].

There is a great deal of interest in new electrochromic materials which exhibits rapid response times, long term stability with high chromatic contrast, good optical memory and chemical stability [35]. Electrochromic response time is the time the polymer takes in response to the potential pulse to go one color state to another. Switching life is related to the ratio of the reduction to the oxidation charges involved in the electrochromic process. The optical memory is the persistence of the colored state even when the driving voltage is removed [36].

Electrochromic anti-glare car rearview windows have already been commercialized with other proposed applications of electrochromic materials including their use in controllable light-reflective or light-transmissive devices for optical information and storage, sunglasses, protective eyewear for the military, controllable aircraft canopies, glare-reduction systems for offices and “smart windows” for use in cars and in buildings [37-39].

1.9.1 Spectroelectrochemistry

In spectroelectrochemistry, chemical changes in the reactant are monitored spectrophotometrically in situ while the electrochemistry is performed. The spectra of electroactive polymers show marked and interesting changes during the redox process, and by monitoring the changes one can arrive at conclusion regarding the mechanism. The potential to the cell is applied from a potentiostat and the current

response is measured simultaneously along with the spectral changes. Because optical absorption is sensitive to even small changes in concentration of the redox species, this is a valuable tool [6]. Spectroelectrochemistry is used to obtain information about the electronic structure of the conducting polymers and to examine the spectral changes that occur during redox switching [40].

1.9.2 Colorimetry

Quantitative measurement of the color of electrochromic polymers is performed by colorimetry analysis. In order to describe the color objectively, a color system was established by The Commission Internationale de l'Eclairge, which is also known as CIE system. This method takes into consideration the response of a standard observer to various color stimuli, the nature of the light source, and the light reflected by the object under study. These functions are used to calculate tristimulus values (XYZ) that define the CIE color spaces [41].

Hue, saturation and luminescence are the parameters which are used to define the color. Hue, which is represented by "a", refers to dominant wavelength or chromatic color. Purity (intensity) of a color is known as the saturation and represented by "b". "L" corresponds to luminance, in other words brightness.

The color space, which is used to determine the color of the copolymers, is illustrated in figure 1.8. On this chart, x-axis corresponds to hue (a), y-axis corresponds to intensity (b) and z-axis corresponds to luminance (L).

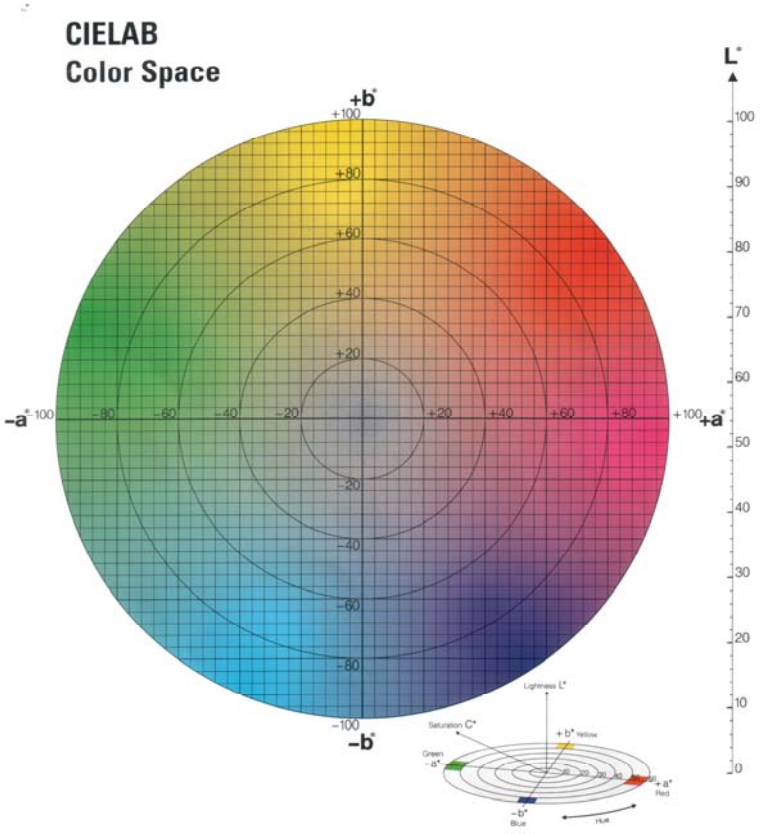

Figure 1.8 CIELAB color space

1.9.3 Switching

One of the most important characteristics of ECDs is the response time needed to perform a switching between two colored states. The other important parameter is the optic contrast, which can be defined as the percent transmittance difference between the redox states. ECDs that switch rapidly and exhibit high contrast ratios (%*T*) are of special interest for use in many applications such as dialed-tint windows, large area displays and automatic dimming mirrors [42].

1.9.4 Open Circuit Memory

The color persistence is an important feature since it is directly related to aspects involved in its utilization and energy consumption during use [43]. Optical memory is the persistence of the colored state even when the driving voltage is removed. For polymer-based electrochromic materials, it is related to the stability in the electrolytic medium of the doped and undoped forms of the polymer [36].

1.9.5 Stability

The stability of the devices towards multiple redox switching usually limits the utility of electrochromic materials in ECD applications. Different applied voltages and environmental conditions of the materials are responsible for the device failure. Therefore, ECDs with good environmental and redox stability are required for future applications [42].

1.10 Electrochromic Devices (ECDs)

An electrochromic device (ECD) is essentially a rechargeable battery in which the electrochromic electrode is separated by a suitable solid or liquid electrolyte from a charge balancing counter electrode, and the color changes occur by charging and discharging the electrochemical cell with applied potential of a few volts [44].

A dual-type ECD consists of two electrochromic materials (one revealing anodic coloration, the other revealing cathodic coloration) deposited on transparent ITO, placed in a position to face each other and a gel electrolyte in between. In order to maintain a balanced number of redox sites for switching, the redox charges of the two complementary polymer films were matched by chronocoulometry. Before constructing the ECD, the anodically coloring polymer film was fully reduced and the cathodically coloring polymer film was fully oxidized. Upon application of voltage,

the doped polymer will be neutralized, whereas the other will be reduced, thus will result in the color change. Schematic representation of devices is given in figure 1.9.

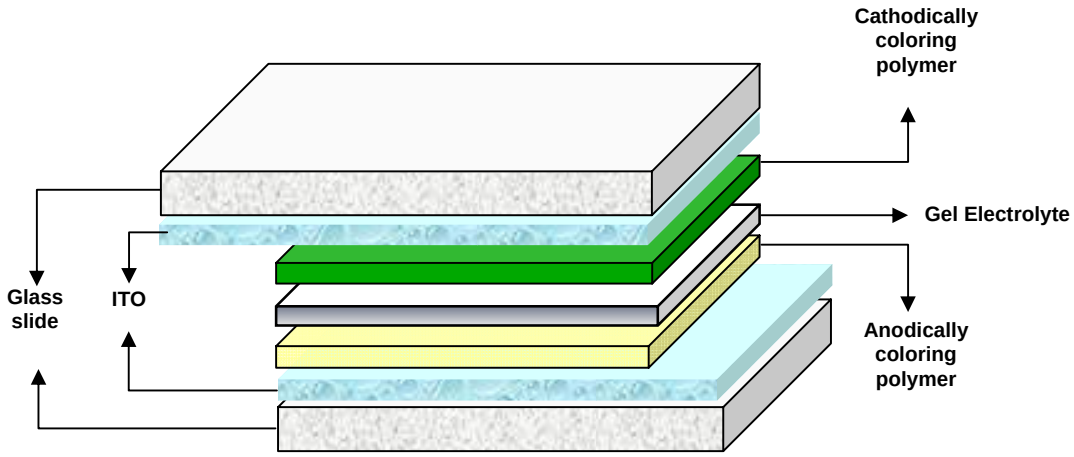

Figure 1.9 Schematic representation of ECDs

Tin doped indium oxide (ITO) is routinely used as an electrode in electrochromic applications due to its unique combination of properties including optical transparency, low electrical resistance and excellent surface adhesion. Cathodically coloring polymer is the one that passes from an almost transparent state to a highly colored state upon reduction of the p-doped form. Poly(isothianaphthene) (PITN) was reported as the first example of a low band gap, cathodically coloring CP [45]. For a number of synthetic and electrochemical reasons, PITN has not found a high level of applicability in ECDs. Recently, poly(3,4-ethylenedioxythiophene) (PEDOT) has emerged as a low band gap (E_g = 1.6 eV, 775 nm), cathodically coloring CP [46]. In addition to its low band gap, PEDOT has a low redox potential, is very stable to multiple redox switching, and has a high conductivity. Ideally, an anodically coloring CP is chosen to have a high band gap (E_g) ≥3.0 eV (<410 nm) with π to π^* electronic transitions extending from the high-energy end of the visible spectrum into the ultraviolet region. In its reduced form, the polymer is transmissive to a major portion of the visible spectrum. Upon oxidation, charge carrier absorptions are induced in the visible region, resulting in an opaque and/or colored state. This

anodically coloring behavior is observed for many of the common conjugated polymers, including poly(*p*-phenylene), polypyrrole, and poly(*p*-phenylene vinylene) [42].

The requirements for high performance electrochromic devices are:

a) High electrochromic efficiency, expressed in $cm^2 C^{-1}$ and related to the injected charge in the material to change its color;

b) Short electronic response time;

c) Good stability;

d) Optical memory, defined as the color stability under open circuit potential conditions;

e) Optical contrast, also called write-erase efficiency

f) Color uniformity [4].

1.11 Aims of the work

- To synthesize 2-benzyl-5,12-dihydro-2*H*-pyrrolo[3',4':2,3][1,4]dioxocino[6,7-*b*] quinoxaline (DPOQ) and 5,12-dihydrothieno[3',4':2,3][1,4]dithiocino[6,7-*b*] quinoxaline (DTTQ) monomers.
- To perform electrochemical synthesis of P(DPOQ-co-BT) and P(DTTQ-co-BT).
- To characterize the copolymer films with various techniques.
- To investigate electrochromic and spectroelectrochemical properties of the polymers.
- To examine their use in electrochromic devices.

CHAPTER II

EXPERIMENTAL

2.1 Chemicals

Chloroform (Merck), dichloromethane (DCM) (Merck), methanol (Merck), acetonitrile (ACN) (Merck), acetone (Merck), HCl (Merck), NaOH (Merck), acetic acid (Merck), potassium hydroxide (Merck), N, N-Dimethylformamide (DMF) (Merck), toluene (Sigma), dry ether (Merck), thionyl chloride (Aldrich), iminodiacetic acid (Fluka), benzyl bromide (Merck), propylene carbonate (PC) (Aldrich) and poly(methyl metacrylate) (PMMA) (Aldrich) were used without further purification. Tetrabutylammonium tetrafluoroborate (TBAFB) (Aldrich), tetrabutylammonium hexafluorophosphate (TBAFP) (Aldrich), 2,2'-bithiophene (BT) (Aldrich), magnesium sulfate (Aldrich), diethyl oxalate (Aldrich), phenylenediamine (Merck), butyllithium (Aldrich), elemental sulfur (Fluka), sodium bicarbonate (Aldrich), potassium carbonate (Fluka) and 3,4-ethylenedioxythiophene (EDOT) (Aldrich) were used as received.

2.2 Instrumentation

2.2.1 Potentiostat

Wenking POS 73 and Solatron 1285 potentiostats were used to supply a constant potential in electrochemical syntheses. A potentiostat is an electronic device

that controls the potential difference between a working electrode and a reference electrode. It does this by injecting current into the cell through the counter electrode. It also minimizes the effect of IR drop by positioning reference electrode close to the working electrode.

Potentiostat requires working, counter and reference electrodes. Electrochemical reactions occur at the working electrode. Its potential is measured with respect to reference electrode, which has constant potential as long as no current flows through it. The current amplifier supplies current to the cell, regardless of the solution resistance. By this way the potential is controlled whereas the current is varied. Basic instrumentation of the potentiostat can be seen in figure 2.1.

2.2.2 Cyclic Voltammetry System

The CV system was used in order to investigate the electroactivity of the polymers and to obtain the oxidation-reduction peak potentials of the monomers. The system consists of a potentiostat, an XY recorder and a CV cell containing ITO coated glass working electrode, platinum wire counter electrode and Ag/Ag^{+} reference electrode. Cyclic voltammetry measurements were carried out by cycling the potential of the working electrode, which is immersed in an unstirred solution, and measuring the resulting current at the working electrode. Wenking POS 73 was used for the cyclic voltammetry experiments.

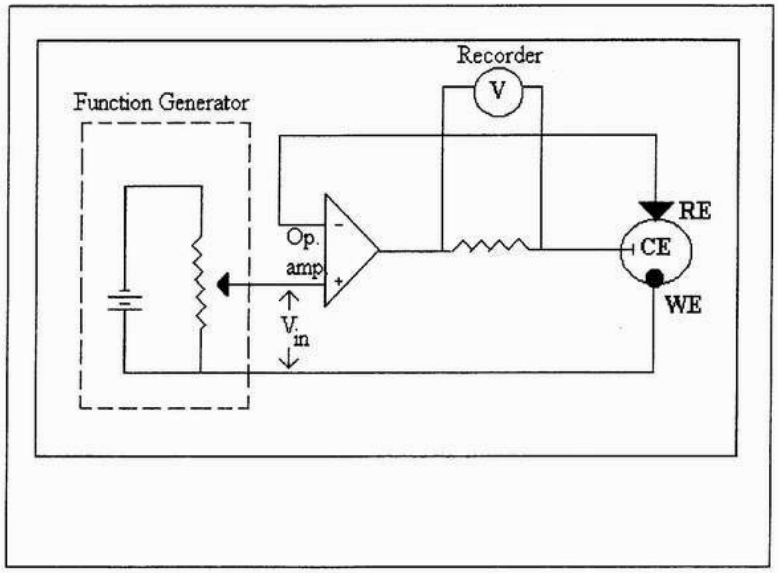

Figure 2.1 Basic Circuit of the Potentiostat

2.2.3 Electrolysis Cell

Electrolyses were performed in a one-compartment cell which has suitable inlets for passing N_2 gas through the solution. The working and counter electrodes were platinum (Pt) and the reference electrode was silver (Ag) wire.

2.2.4 Nuclear Magnetic Resonance Spectrometer (NMR)

NMR spectra of the monomers were recorded on a Bruker-Instrument-NMR Spectrometer (DPX-400) by using $CDCl_3$ as the solvent and tetramethylsilane as the internal standard relative to which the chemical shifts (δ) are given.

2.2.5 Fourier Transform Infrared Spectrometer (FTIR)

All the monomer and copolymer samples were transformed into KBr pellets and all the spectra were recorded by using a Nicolet 510 FTIR spectrometer for the detection of functional groups.

2.2.6 Scanning Electron Microscope (SEM)

The surface morphologies of the copolymer films were analyzed by using JEOL JSM-6400 scanning electron microscope.

2.2.7 Four-Probe Conductivity Measurements

Four-probe technique was used for conductivity measurements. It gives more reliable and rapid results compared to two probe technique. This technique eliminates errors caused by contact resistance, since the two contacts measuring the voltage drop are different from the contacts applying the current across the sample.

Figure 2.2 shows the simplest form of a four-point probe measurement setup which consists of four equally spaced osmium metal tips placed on a head. Sample is put on the flat region and the head is lowered until the probes touch the sample. A direct current is passed through the specimen between the outer probes and resulting potential difference is measured between the inner probes.

The conductivity is determined by the equation below:

$$\sigma = \ln 2 / (\pi d \times i / V)$$

σ: Conductivity

i: current applied through the outer probes

V: voltage drop measured across the inner probes

d: sample thickness

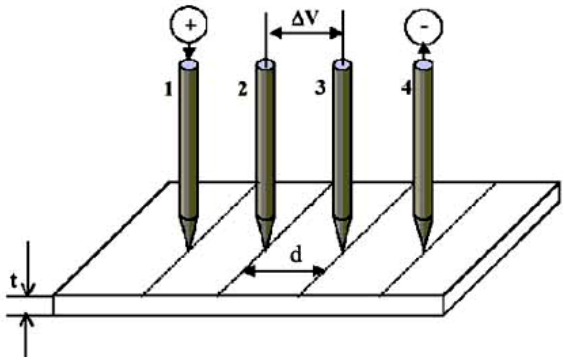

Figure 2.2 Schematic representation of the four-probe device

2.2.8 UV-Vis Spectrophotometer

Agilent 8453 UV-Vis spectrophotometer was used in order to carry out spectroelectrochemical studies.

2.2.9 Colorimetry Measurements

Colorimetry measurements were performed by using the Coloreye XTH Spectrophotometer (GretagMacbeth).

2.3 Procedure

2.3.1 Synthesis of 2-benzyl-5,12-dihydro-2*H*-pyrrolo[3',4':2,3][1,4]dioxocino[6,7-b] quinoxaline (DPOQ)

2.3.1.1. Synthesis of dimethyl iminodiacetate

Iminodiacetic acid (10.0 g, 0.075 mol) was dissolved in 400 mL methanol. 20 mL thionyl chloride were added dropwise to this mixture by cooling in ice bath. A vigorous and exothermic reaction took place. The solution was refluxed for 7 hours at 65 °C, the solution was cooled and the solvent was removed over rotatory evaporator. A white colored solid product was obtained. It was dissolved in water and a dilute solution of potassium hydroxide was added in small portions until the solution became slightly basic. Organic material was extracted with dichloromethane three times (3x75 mL). The organic layer was dried over $MgSO_4$ and the solvent was removed over rotatory evaporator. A light colored oily liquid was obtained with 69% yield (8.36 g).

2.3.1.2. Synthesis of dimethyl N-benzyliminodiacetate

A mixture of dimethyl iminodiacetate (13.0 g, 0.081 mol), $NaHCO_3$ (16.3 g, 0.194 mol) and 40 mL DMF were placed in a round bottomed flask. Benzyl bromide (13.8 g, 0.081 mol) was added dropwise and the mixture was refluxed for 24 hours at 40 °C until the CO_2 evolution stopped. The cooled reaction mixture was poured into 100 g ice-water mixture. The product was extracted with toluene (5x10 mL) and dried over $MgSO_4$. Then it was filtered and the solvent was removed over rotatory evaporator. The resulting product was yellow oil with 90% yield (18.3 g).

2.3.1.3. Synthesis of dimethyl 1-benzyl-3,4-dihydroxy-1H-pyrrole-2,5-dicarboxylate

Sodium (1.5 g, 0.065 mol) was added into 25 mL methanol in a three necked flask under nitrogen atmosphere. Dimethyl N-benzyliminodiacetate (7.0g, 0.028 mol) and 4 mL (0.029 mol) diethyl oxalate in methanol were dropwise added. The addition was performed in an ice bath. Then, the reaction mixture was refluxed for 18 hours, and after cooling to room temperature, the mixture was poured into 100 mL ice water. After waiting for a few hours, the pH of the mixture was adjusted to 5 by adding acetic acid. The crude solid product was filtered and recrystallized from acetone. The light yellow crystals were obtained with 50% yield (4.3 g).

2.3.1.4. Synthesis of 2,3-bis(bromomethyl) quinoxaline

Phenylenediamine (2.2 g, 0.020 mol) and 1,4-dibromo-2,3-butanedione (5.0 g, 0.020 mol) were dissolved separately in ethanol and mixed, then stirred for 1 hour at 0 °C. After cooling the solution in a deep freeze, crystalline 2,3-bis(bromomethyl)quinoxaline (5.7 g) was obtained in 90% yield.

A mixture of 2,3-bis(bromomethyl)quinoxaline (0.50 g, 1.58 mmol) and K_2CO_3 (0.45 g, 3.26 mmol) were added into dimethyl 1-benzyl-3,4-dihydroxy-1*H*-pyrrole-2,5-dicarboxylate (0.50 g, 1.64 mmol) solution in 20 ml DMF. The mixture

was heated at 120 °C by vigorously stirring for 1 hour, and then cooled solution was poured into cold water. The light brown solid was filtered and dried. The yield was 76% (0.57 g).

0.5 g of resultant cyclic product were heated for one night with 5 mL 2.5 N NaOH solution, into which 3-5 drops of ethanol had been added. The excess alcohol was distilled (the mixture was not dried). The resulting oily mixture was dissolved in water and washed with chloroform. The ice cooled water phase was acidified with concentrated HCl. The precipitated gray solids were filtered, dried and the dicarboxylic acid derivative was added into boiling ethanolamine (5 mL). After completion of CO_2 evolution, the mixture was poured into cold water and extracted with dichloromethane. The organic phase was dried and the solvent was removed. Crystalline solid with 20% yield (0.075 g) was obtained. Route for synthesis of the monomer is shown in figures 2.3 (a), 2.3 (b) and 2.3 (c).

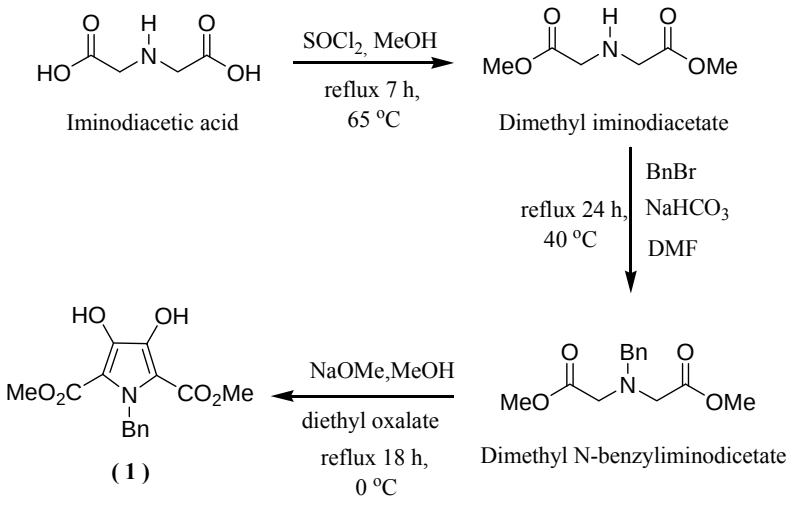

Figure 2.3 (a) Synthesis of dimethyl 1-benzyl-3,4-dihydroxy-1*H*-pyrrole-2,5-dicarboxylate

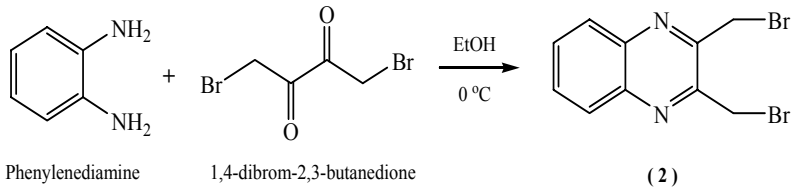

Figure 2.3 (b) Synthesis of 1,2-dibromomethyl quinoxaline

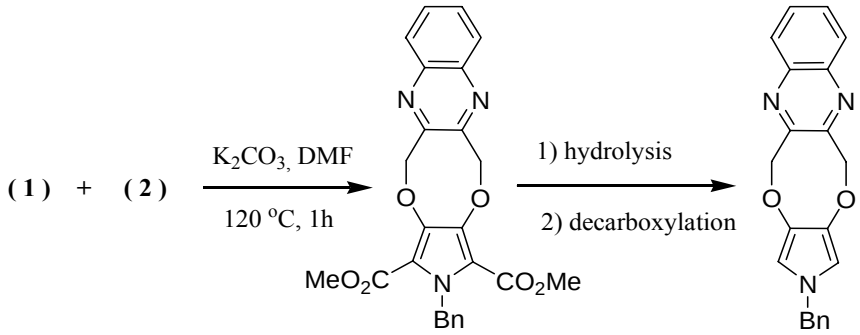

Figure 2.3 (c) Synthesis of DPOQ

2.3.2. Synthesis of 5,12-dihydrothieno[3',4':2,3][1,4]dithiocino[6,7-b] quinoxaline (DTTQ)

2.3.2.1. Synthesis of tetrabromothiophene

22 mL (4.0 mol) Br_2 were slowly added into the mixture of 8 mL (8.4 g, 0.1 mol) thiophene and 3 mL $CHCl_3$ in 2 hours on an ice bath. The reaction mixture was refluxed for 5 hours. After the mixture was cooled, 5 mL 2 N NaOH were added and vigorously stirred for 0.5 h. The solid product was separated, washed with water and crystallized over hot $CHCl_3$. The white crystals were obtained with 78% yield (31.0 g).

2.3.2.2. Synthesis of 3,4–dibromothiophene

11.2 g zinc dust were placed into a two necked round bottom flask. 20 mL CH_3COOH and 40 mL water were added. The mixture was heated until boiling and tetrabromothiophene (30 g, 0.075 mol) was added in 1 hour in small portions while the mixture was still heated. Then, 20 mL water were added into the flask and distillation was performed. The distilled part was placed into a separatory funnel and the organic product was taken into the ether phase. CH_3COOH was removed by washing the ether phase with water, Na_2CO_3 and then water again. Ether was removed over rotatory evaporator. Monobromothiophene and 3,4–dibromothiophene were obtained via vacuum (15 mmHg) distillation at 60-80 °C and 110-120 °C, respectively. The yield was 83% (15.1 g).

3,4-Dibromothiophene (0.50 g, 2.07 mol) was dissolved in 5 ml dry ether and cooled with dry-ice/acetone mixture to -78 °C. BuLi solution in ether (0.9 mL) was added slowly in 20 min, and the mixture was stirred for 0.5 h. After that, elemental sulfur (0.13 g, 0.507 mmol) was added to the mixture at once and stirred for 0.5 h at -78 °C. The same procedure was repeated again; BuLi (0.9 ml) added above the mixture in 15 min. and stirred for 0.5 h. Then, elemental sulfur (0.13 g, 0.507 mmol) was added to the mixture at once and stirred for another 0.5 h at -78 °C. After this step, the mixture was stirred at room temperature for 3 hours. 2,3–Bis(bromomethyl) quinoxaline (0.71 g, 2.25 mmol) was added slowly into the mixture at 0 °C and stirred for one night at room temperature. It was poured into water and a black solution was obtained. Organic material was extracted with dichloromethane and dried over $MgSO_4$. The solvent was removed and the black oily liquid was purified with column chromatography (Silica gel 60; hexane/ethyl acetate 5:1). A light yellow solid was obtained with 56.8 % yield (1.21 g). The synthesis route of the monomer is shown in figure 2.4.

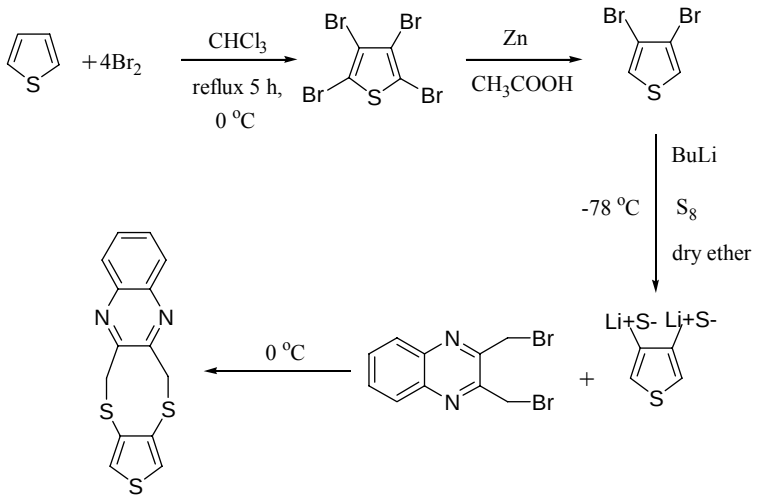

Figure 2.4 Synthesis route of DTTQ

2.3.3 Synthesis of Copolymers of DPOQ with Bithiophene, P(DPOQ-co-BT)

The copolymerization of DPOQ with bithiophene was performed via constant potential electrolysis at +1.5 V under nitrogen atmosphere in a one compartment cell where the working and counter electrodes were Pt foils and the reference electrode was Ag/Ag^+. 0.01 M DPOQ and 0.01 M bithiophene were dissolved in ACN/TBAFB (0.1 M) solvent-electrolyte couple. In order to remove excess TBAFB and unreacted monomer, films were washed several times with ACN. For the spectroelectrochemistry and kinetic studies, the copolymer was coated on ITO coated glass slide by using the same system.

2.3.4 Synthesis of Copolymers of DTTQ with Bithiophene, P(DTTQ-co-BT)

The copolymer of DTTQ with bithiophene was synthesized by sweeping the potential between 0.0 V and +2.0 V with 500 mV/sec scan rate in a solution containing 0.01 M DTTQ, 0.01 M bithiophene in DCM/TBAFP (0.1 M) solvent-electrolyte couple. The working and counter electrodes were Pt foils and the reference electrode was Ag/Ag^+. Films were washed with DCM in order to remove excess TBAFP and unreacted monomer after the potentiodynamic electrochemical

polymerization. Similar system was used to synthesize the copolymer on ITO glass slide.

2.3.5 Spectroelectrochemical Studies

Spectroelectrochemical studies of the copolymers were performed in a UV cuvette by using ITO-coated glass as working, Pt wire as counter, and Ag/Ag^{+} as reference electrodes. The samples were deposited as thin films on ITO-coated glass in a solution containing 0.01 M DPOQ with 0.01 M bithiophene in the presence of ACN/TBAFB (0.1 M) at +1.5 V. Spectroelectrochemical series were taken while different potentials were applied to coated ITO slides in a monomer free solution.

P(DTTQ-co-BT) film was potentiodynamically synthesized on ITO electrode in the presence of 0.01 M DTTQ and 0.01 M bithiophene, while the potential was swept between 0.0 V and +2.0 V in DCM/TBAFP (0.1 M).

2.3.6 Switching Studies

Chronoabsorptometry, a square wave potential step method coupled with optical spectroscopy, is used to evaluate the response time of the device. The potential was set at an initial potential for a residence time of 5 s and than a second potential was applied for the same set period of time until being switched back to the initial potential again. Applied potentials were determined from the spectroelectrochemical studies, where the ultimate states of the devices were achieved. The dynamic electrochromic experiments for P(DPOQ-co-BT) and P(DTTQ-co-BT) were carried out at 455 and 485 nm, respectively. For P(DPOQ-co-BT), the voltage was switched between +0.5 V and +1.4 V with a residence time of 5 seconds in a solution of ACN/TBAFB (0.1 M) and for the copolymer of DTTQ with BT, the voltage was switched between +0.3 V and +1.3 V with a residence time of 5 seconds in a solution of DCM/TBAFP (0.1 M).

2.3.7 Colorimetry Studies

In order to define and compare the colors of the polymers, colorimetry studies were performed. After synthesizing P(DPOQ-co-BT) and P(DTTQ-co-BT) films on ITO electrodes, they were placed into monomer free solutions containing ACN/TBAFB (0.1 M) and DCM/TBAFP (0.1 M), respectively. Three attributes of color; hue (a), saturation (b) and luminance (L) were measured.

2.3.8 Electrochromic Device (ECD) Studies

Solatron 1285 model potentiostat/galvanostat was used for coating polymers on ITO-glass electrode. Poly (3,4-ethylenedioxythiophene) (PEDOT) was potentiostatically deposited on ITO working electrode by applying +1.5 V in ACN/TBAFB (0.1 M) solvent-electrolyte system. P(DPOQ-co-BT) film was coated on ITO electrode potentiostatically at +1.5 V in a solution containing 0.01 M DPOQ with 0.01 M bithiophene in the presence of ACN/TBAFB (0.1 M). Coating of P(DTTQ-co-BT) film on ITO electrode was performed via cyclic voltammetry, scanning between 0.0 V and +2.0 V in a solution containing 0.01 M DTTQ with 0.01 M BT in the presence of DCM/TBAFP (0.1 M). By sandwiching the gel electrolyte between the anodically coloring polymer and the cathodically coloring polymer, the device was constructed.

2.3.8.1 Gel Electrolyte Preparation

Gel electrolyte was prepared by using TBAFB:ACN:PMMA:PC in the ratio of 3:70:7:20 by weight. After TBAFB was dissolved in ACN, PMMA was added into the solution. In order to dissolve PMMA, vigorous stirring and heating was required. PC, as a plasticizer, was introduced to the reaction medium when all of the PMMA was completely dissolved. The mixture was stirred and heated until the highly conducting transparent gel was produced [47].

2.3.8.2 Spectroelectrochemical studies of devices

Spectroelectrochemical studies of P(DPOQ-co-BT)/PEDOT and P(DTTQ-co-BT)/PEDOT devices were performed by applying the potentials from 0.0 V to + 1.8 V and UV-VIS spectra series were obtained.

2.3.8.3 Switching studies of devices

The experiments were carried out at 612 and 606 nm for P(DPOQ-co-BT)/PEDOT and P(DTTQ-co-BT)/PEDOT devices, respectively where the maximum transmittance difference between redox states were observed in the visible region. Both of the P(DPOQ-co-BT)/PEDOT and P(DTTQ-co-BT)/PEDOT devices were switched between 0.0 V and +1.8 V with a residence time of 5 seconds.

2.3.8.4 Stability of devices

Cyclic voltammetry technique was used for the stability experiments of the devices. The potential was cycled between 0.0 and +1.8 V with 500 mV/s scan rate.

2.3.8.5 Open Circuit Memory Studies

To test the open circuit memory of the devices, potential was applied for one second and the device was left under open circuit conditions for 100 s while monitoring the percent transmittance change at a fixed wavelength. The open circuit memory of P(DPOQ-co-BT)/PEDOT device was tested at 0.0 V and +1.8 V at 455 nm and P(DTTQ-co-BT)/PEDOT device at 0.0 V and +1.8 V at 485 nm.

CHAPTER III

RESULTS AND DISCUSSION

3.1 Characterization of monomers by ^{1}H-NMR Spectroscopy

NMR spectra of monomer were taken by using $CDCl_3$ as the solvent and chemical shifts (δ) are given relative to tetramethylsilane as the internal standard.

^{1}H NMR ($CDCl_3$) of monomer DPOQ: (δ,ppm): 8.00 (dd, benzene), 7.69 (dd, benzene), 5.53 (s, CH_2–O), 6.17 (s, pyrrole), 4.72 (s, N–CH_2), 7.20 (dt, benzene), 7.00 (dd, benzene), 7.20 (s, $CDCl_3$) (Figure 3.1(a)). [M^+] was observed at m/z 343.10.

^{1}H NMR ($CDCl_3$) of monomer DTTQ: (δ,ppm): 7.91 (dd, benzene), 7.62 (dd, benzene), 4.35 (s, CH_2–S), 7.18 (s, thiophene), 7.43 (s, $CDCl_3$) (Figure 3.1(b)). [M^+] was observed at m/z 302.00

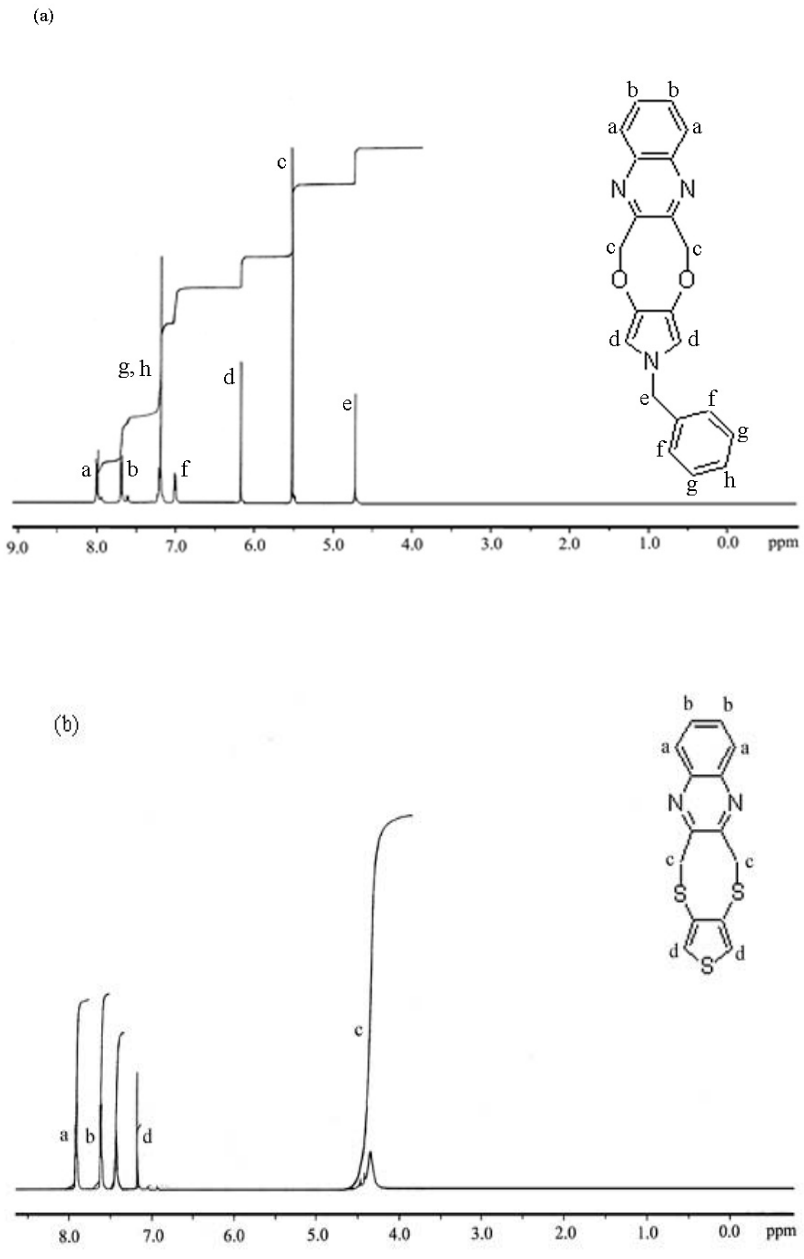

Figure 3.1 ^{1}H NMR spectrum of (a) DPOQ and (b) DTTQ

3.2 FTIR Spectra

FTIR spectrum of the DPOQ monomer (Figure 3.2 (a)) shows the following absorption peaks: 3061 cm^{-1} (C–H_α stretching, pyrrole), 3126 cm^{-1} (aromatic C–H), 2928 cm^{-1} (aliphatic C–H), 1564,1543 cm^{-1} (C=N stretching), 1487-1353 cm^{-1} (aromatic C=C, C–N stretching due to pyrrole and benzene), 1157 cm^{-1} (C–O–C stretching), 1045 cm^{-1} (C–H in plane bending of benzene), 763 cm^{-1} (C–H_α out of plane bending of pyrrole) and 731 cm^{-1} (monosubstituted benzene).

Most of the characteristic peaks of the monomer DPOQ remained unperturbed upon copolymerization with bithiophene (Figure 3.2 (b)). The intensity absorption bands of the momomer at 3061 and 763 cm^{-1} arising from C–H_α stretching and out of plane bending of pyrrole moiety, respectively, disappeared completely. This is an evidence of the polymerization from 2,5 positions of pyrrole moiety of the monomer. Whereas, two new bands related to C–H_β out-of-plane bending of 2,5 disubstituted bithiophene and C–S stretching appeared at 793 and 632 cm^{-1}, respectively [48]. The broad band observed at around 1640 cm^{-1} proves the presence of polyconjugation and the new peak at 1076 cm^{-1} indicates the presence of the dopant ion (BF_4^-).

In FTIR spectrum of the DTTQ monomer (Figure 3.2 (c)) the following absorption bands arise: 3020 cm^{-1} (C–H_α stretching of thiophene), 3093 cm^{-1} (aromatic C–H), 2958 cm^{-1} (aliphatic C–H), 1558 cm^{-1} (C=N stretching), 1483-1359 cm^{-1} (aromatic C=C stretching), 1157, 1097 (C–H in plane bending of benzene and thiophene), 766 cm^{-1} (C–H_α out of plane bending of thiophene), 692 cm^{-1} (C–S–C stretching).

FTIR spectra of electrochemically synthesized P(DTTQ-co-BT) showed the characteristic peaks of the monomer (Figure 3.2 (d)). The peaks related to C–H_α stretching of thiophene disappeared completely. On the other hand, evolution of a new peak was observed at 795 cm^{-1}, which is attributed to the C–H_β out-of-plane bending of 2,5 disubstituted bithiophene. The new broad band at around 1640 cm^{-1} was due to polyconjugation. The strong absorption peak at 849 cm^{-1} was attributed to the incorporation PF_6^- ions into the polymer film during doping process. Results of

the FTIR studies clearly indicated the copolymerization of the monomers with bithiophene.

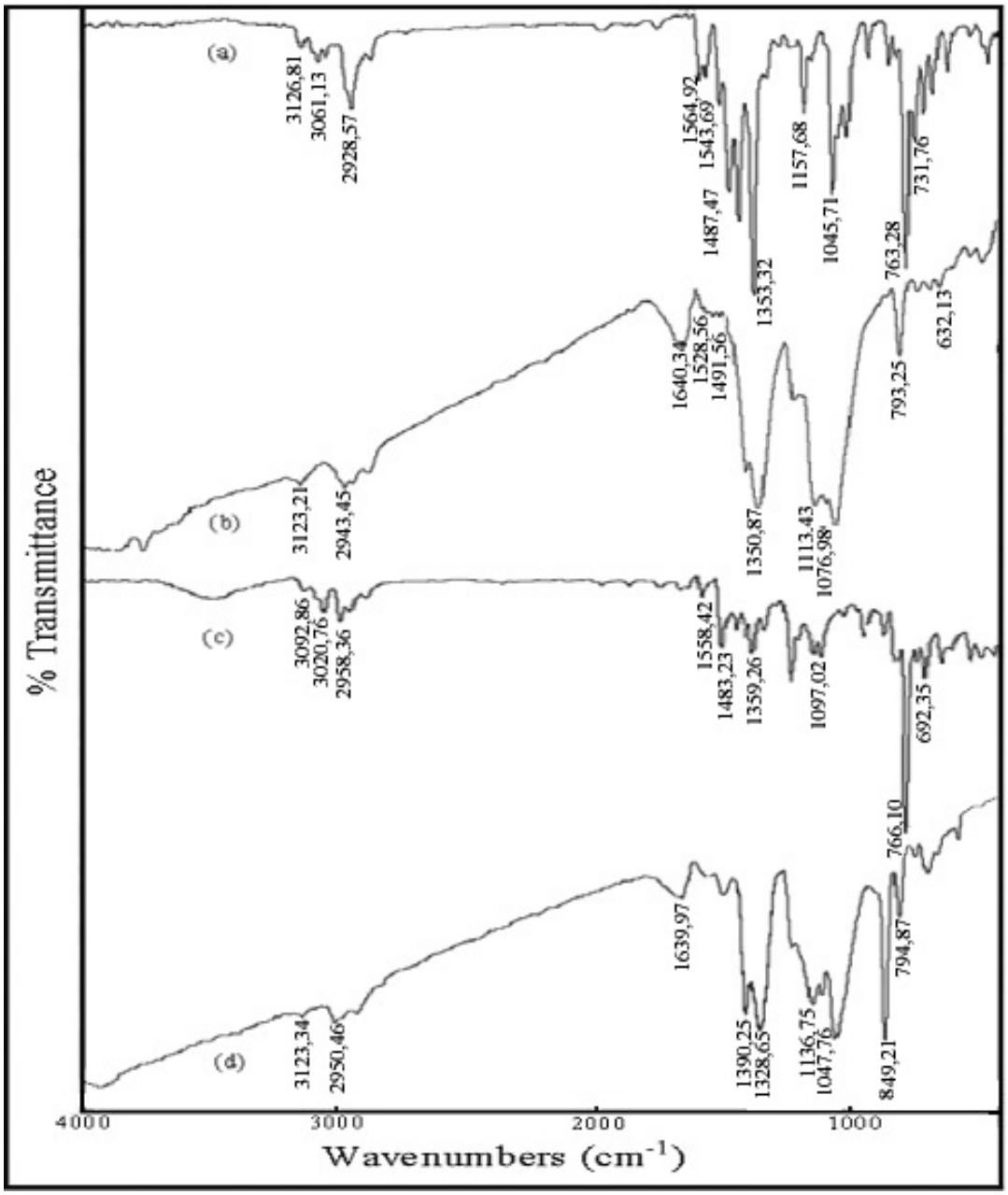

Figure 3.2 FTIR spectrum of (a) DPOQ, (b) P(DPOQ-co-BT), (c) DTTQ, (d) P(DTTQ-co-BT)

3.3. Cyclic Voltammograms

CV of the DPOQ showed two oxidation peaks at +0.46 V and +0.74 V and a reduction peak at +0.3 V, which imply the electroactivity of the monomer (Figure 3.3 (a)). An increase in the peak intensities was observed upon sequential cycles. However, leakage of the homopolymer from the electrode surface was observed which may due to formation of stable radical cations [49]. After addition of bithiophene into the solution, the electroactive copolymer formation on the electrode surface with an oxidation peak at +0.60 V and a reduction peak at +0.44 V was observed (Figure 3.3 (b)). This redox behavior and the increments between consecutive cycles were completely different than those of both monomer and pure bithiophene (Figure 3.3 (c)) (pure bithiophene in ACN/TBAFB (0.1 M)– $E_{p,a}$: +1.07 V and $E_{p,c}$: +0.67 V).

As seen from Figure 3.3 (d), the DTTQ exhibited electroactivity by revealing one irreversible oxidation peak at +1.62 V. A decrease in peak intensities was observed upon continuous scan which resulted a loss of electroactivity. The CV of DTTQ in the presence of bithiophene was found to be different than those of both monomer and pure bithiophene in terms of both redox behavior ($E_{p,a}$: +1.27 V and $E_{p,c}$: +0.31 V) (Figure 3.3 (e)). Pure bithiophene in DCM/TBAFP (0.1 M) reveals an oxidation peak at +1.10 V and a reduction peak at +0.67 V (Figure 3.3 (f)).

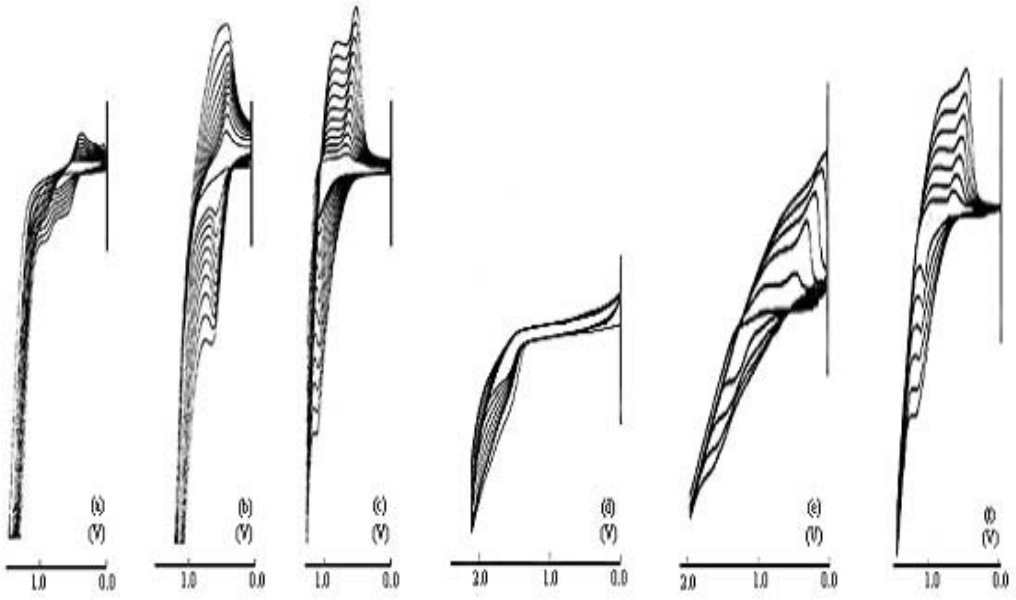

Figure 3.3 Cyclic voltammogram of (a) DPOQ, (b) DPOQ in the presence of bithiophene, (c) pure bithiophene, in ACN/TBAFB (0.1 M) (d) DTTQ, (e) DTTQ in the presence of bithiophene, (f) pure bithiophene, in DCM/TBAFB (0.1 M) on ITO working electrode with 500 mV/s scan rate

3.4. Conductivity Measurements

Electrical conductivity measurements were carried out by using four-point probe technique. The conductivities of P(DPOQ-co-BT) and P(DTTQ-co-BT) films were measured as 0.1 and 0.3 S/cm, respectively.

3.5. Scanning Electron Micrographs

The solution side of the P(DPOQ-co-BT) film revealed a porous-like surface structure (Figure 3.4 (a)) while P(DTTQ-co-BT) film showed a rather coarse structure (Figure 3.4(b)) which were significantly different than that of the granular-like structure of pure polybithiophene (Figure 3.4 (c)). These completely different

morphologies indicate the formation of a new material other than the monomers and bithiophene.

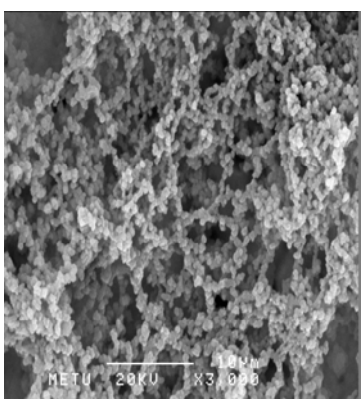

(a)

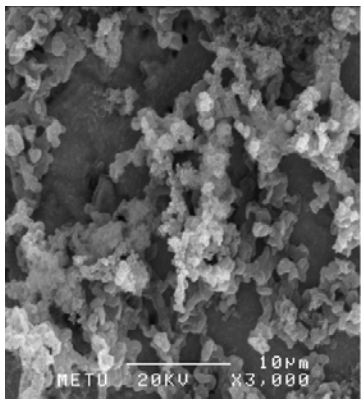

(b)

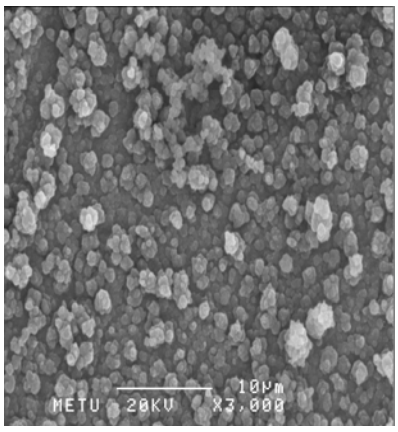

(c)

Figure 3.4 SEM micrographs of solution sides of (a) P(DPOQ-co-BT), (b) P(DTTQ-co-BT) and (c) pure polybithiophene

3.6. Electrochromic Properties of Conducting Polymers

3.6.1 Spectroelectrochemistry

Spectroelectrochemistry studies were performed in order to elucidate electronic transitions during redox switching of the polymers. P(DPOQ-co-BT) coated ITO was switched between +0.5 V and +1.4 V in a monomer free

ACN/TBAFB system in order to obtain the UV-Vis spectra series. The electronic band gap (E_g) was found to be 1.89 eV and λmax value was 455 nm at 0.5 V (Figure 3.5 (a)). Upon oxidation of the polymer, the intensity of the π-π^* transitions reduced and the formation of the charge carrier bands beyond 800 nm were observed while the color of the polymer changed from orange to blue.

The spectroelectrochemical and electrochromic properties of the P(DTTQ-co-BT) were studied by applying potentials ranging from +0.3 V and +1.3 V in monomer free DCM/TBAFP (0.1 M) system. At the neutral state λmax value due to the π-π^* transition of the copolymer was found to be 485 nm and E_g was calculated as 1.81 eV (Figure 3.5 (b)). The film was switched between a red color in the reduced state and blue color in the oxidized state. Upon applied voltage, evolutions of new absorption bands were observed.

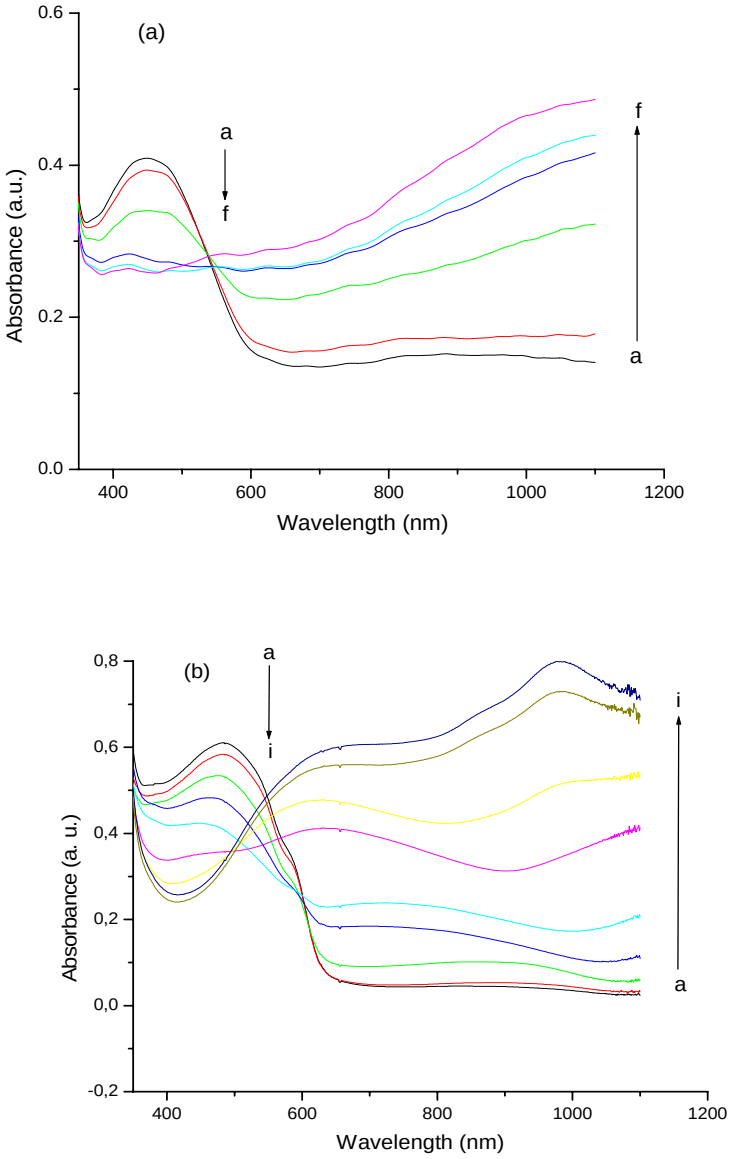

Figure 3.5 Optoelectrochemical spectrum of (a) P(DPOQ-co-BT) as applied potentials between +0.5 V and +1.4 V in ACN/TBAFB (0.1 M); (a) +0.5 V, (b) +0.7 V, (c) +0.9 V, (d) +1.1 V, (e) +1.2 V, (f) +1.4 V. (b) P(DTTQ-co-BT) as applied potentials between +0.3 V and +1.3 V in DCM/TBAFP (0.1 M); (a) +0.3 V, (b) +0.4 V, (c) +0.6 V, (d) +0.7 V, (e) +0.8 V, (f) +0.9 V, (g) +1.0 V, (h) +1.2 V, (i) +1.3 V

3.6.2 Colorimetry

The P(DPOQ-co-BT) film switches between blue color (in the oxidized state) and orange (in the reduced state). P(DTTQ-co-BT) film changes color from red to blue during oxidation. L*a*b values of the films were measured at the fully oxidized and the fully reduced states and the results were recorded in Table 1.

Table 3.1 Electrochromic Properties of Polymers

Material	**Color (ox)**	**Color (red)**	**λmax (nm)**	**L**	**a**	**b**	**Eg (eV)**
PBT	Blue	Orange- red	477	ox: 77 red: 60	ox: -11 red: 10	ox: -30 red: 22	1.85
P(DPOQ-co-BT)	Blue	Orange	455	ox : 56 red: 47	ox : -2 red: 14	ox : -3 red: 33	1.89
P(DTTQ-co-BT)	Blue	Red	485	ox : 43 red: 38	ox : -1 red: 41	ox : -8 red: 30	1.81

ox: oxidized state
red: reduced state

Colors of the P(DPOQ-co-BT) and P(DTTQ-co-BT) at their extreme states are given in figure 3.6.

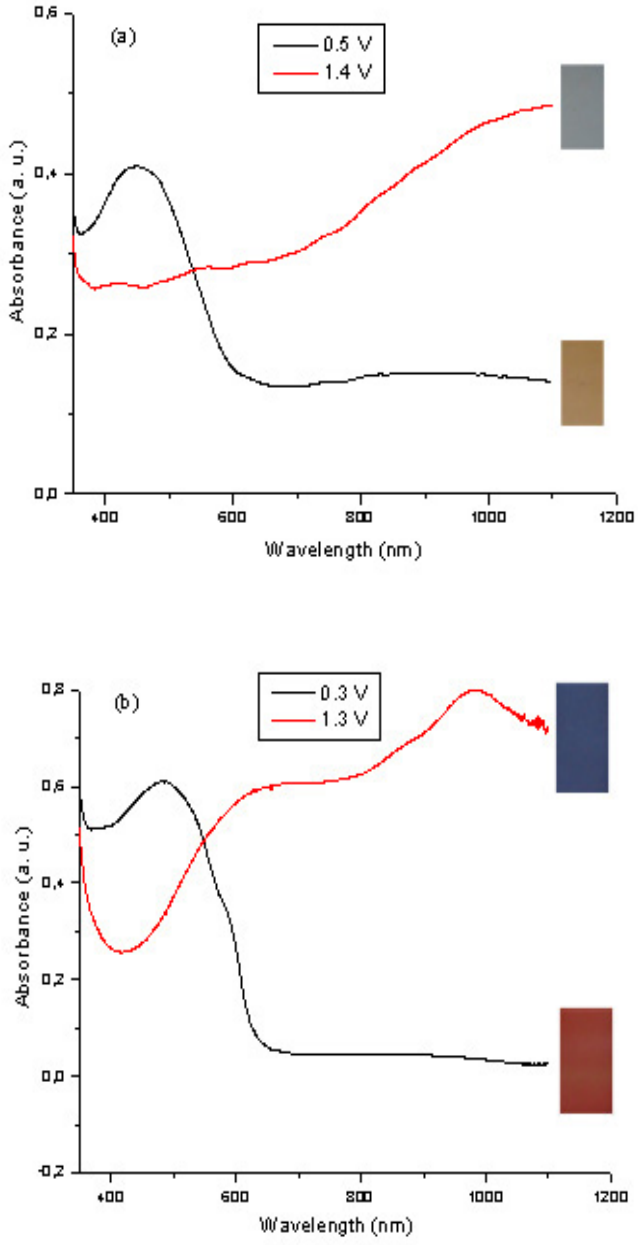

Figure 3.6 Extreme states of (a) P(DPOQ-co-BT), (b) P(DTTQ-co-BT)

3.6.3 Electrochromic Switching

Spectroelectrochemistry studies showed the ability of the copolymers to switch between their redox states with a change in transmittance at a fixed wavelength. Experiments for P(DPOQ-co-BT) were carried out at 455 via switching the potential between +0.5 V and +1.4 V with a residence time of 5 seconds in a solution of ACN/TBAFB (0.1 M). For the copolymer of DTTQ with BT, the voltage was switched between +0.3 V and +1.3 V with a residence time of 5 seconds in a solution of DCM/TBAFP (0.1 M) at 485 nm. Optical contrast and the time needed to reach 95% of the total transmittance change for the copolymers were measured. P(DPOQ-co-BT) was found to have 10.7 % optical contrast with a switching time of 2.0 s (Figure 3.7 (a)) while P(DTTQ-co-BT) exhibited 25.8 % optical contrast with a switching time of 1.3 s (Figure 3.7 (b)).

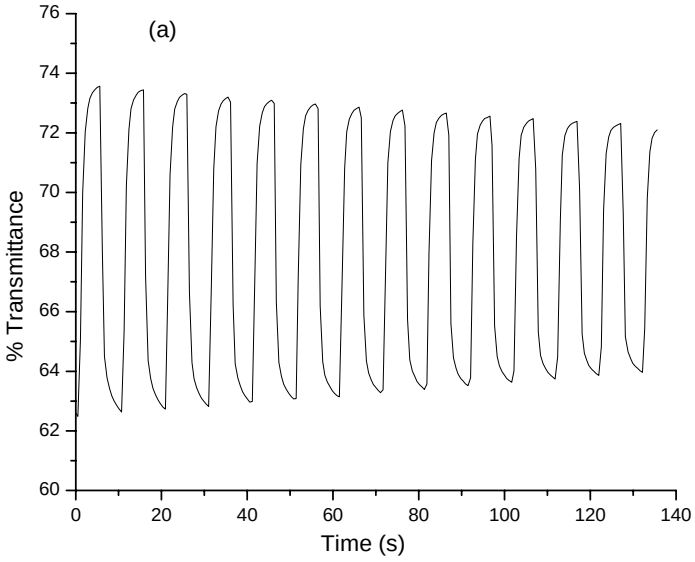

Figure 3.7 Dynamic electrochromic study of (a) P(DPOQ-co-BT) at 455 nm in ACN/TBAFB (0.1 M)

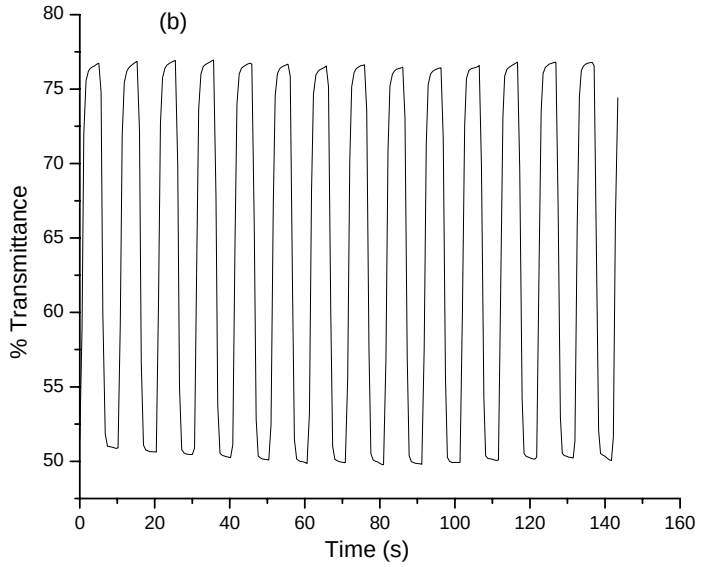

Figure 3.7 Dynamic electrochromic study of (b) P(DTTQ-co-BT) at 485 nm in DCM/TBAFP (0.1 M)

3.7 Electrochromic Devices

A dual-type ECD consists of two electrochromic materials (one revealing anodic coloration, the other revealing cathodic coloration) deposited on transparent ITO, placed in a position to face each other and a gel electrolyte in between. Before constructing the ECD, the anodically coloring polymer films P(DTTQ-co-BT) and P(DPOQ-co-BT) were fully reduced and the cathodically coloring polymer (PEDOT) was fully oxidized. Upon application of the potential, the doped polymer will be neutralized with concurrent oxidation of the complementary polymer, including color formation.

3.7.1 Spectroelectrochemistry of ECDs

Optoelectrochemical spectrum of P(DPOQ-co-BT)/PEDOT device at potentials varying between 0.0 V and +1.8 V is shown in figure 3.8 (a). At 0.0 V, the anodically coloring polymer dominated the device revealing λ_{max} at 467 nm with an

orange color. At this voltage PEDOT was in its oxidized state, exhibiting a transmissive sky blue color. Upon increase in the applied potential, a second absorption at around 800 nm was observed which was an indication of the charge carrier band formation. Further increase resulted in the formation of a new band at 613 nm due to reduction of PEDOT. At +1.8 V, PEDOT was in its most reduced state and the blue color of the polymer was dominated. Thus, upon varying the applied potential from 0.0 V to +1.8 V, the color change from orange to blue was observed.

Similar behavior was observed for P(DTTQ-co-BT)/PEDOT, which showed the maximum absorption at 495 nm, revealing red color at 0.0 V due to P(DTTQ-co-BT) layer. Upon stepwise increase of the applied potential from 0.0 V to +1.8 V, charge carrier band formation and color changed from red to blue were observed. At +1.8 V, PEDOT layer was in its reduced state revealing the π-π^* transition at 606 nm (Figure 3.8 (b))

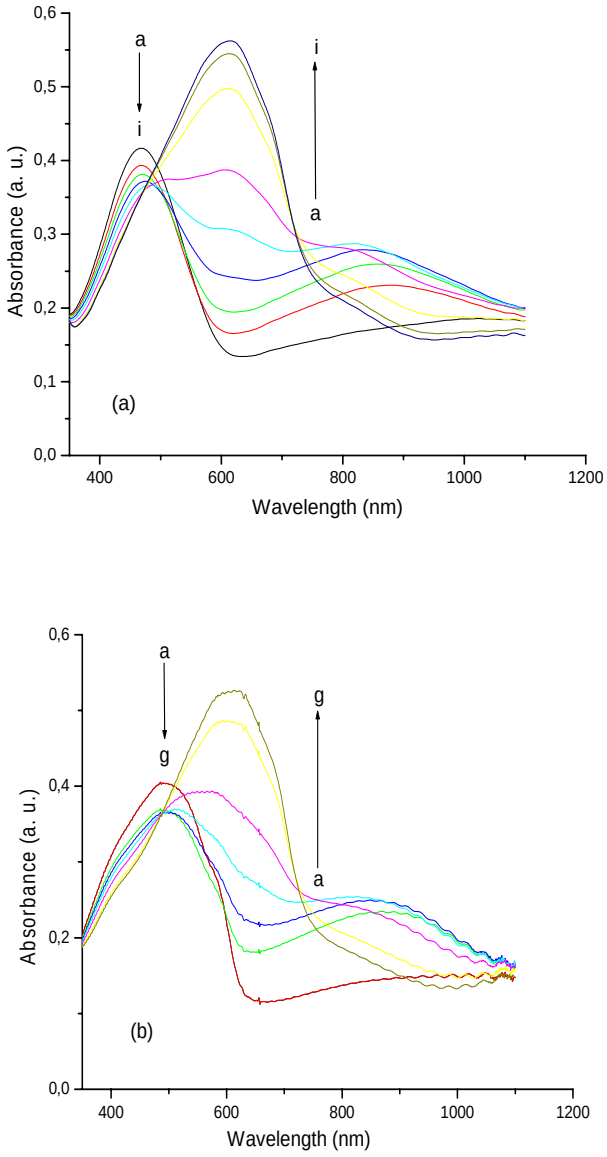

Figure 3.8 Optoelectrochemical spectrum of (a) P(DPOQ-co-BT)/PEDOT ECD at applied potentials between 0.0 V and +1.8 V; (a) 0.0 V, (b) +0.6 V, (c) +0.8 V, (d) +1.0 V, (e) +1.2 V, (f) +1.4 V, (g) +1.6 V, (h) +1.7 V, (i) +1.8 V. (b) P(DTTQ-co-BT)/PEDOT ECD at applied potentials between 0.0 V and +1.8 V; (a) 0.0 V, (b) +0.8 V, (c) +1.0 V, (d) +1.2 V, (e) +1.4 V, (f) +1.6 V, (g) +1.8 V

3.7.2 Switching of ECDs

The switching characteristics of ECDs were investigated at the maximum contrast wavelength during repeated redox stepping experiments. Both of the devices were switched between 0.0 V and +1.8 V. The maximum transmittance difference between the oxidized and reduced states was measured as 29.3 % and 24.9% for P(DPOQ-co-BT)/PEDOT and P(DTTQ-co-BT)/PEDOT devices, respectively. The time required to attain 95% of the total transmittance difference, was found as 1.2 s for P(DPOQ-co-BT)/PEDOT device and 1.0 s for P(DTTQ-co-BT)/PEDOT device (Figure 3.9 (a)-(b)).

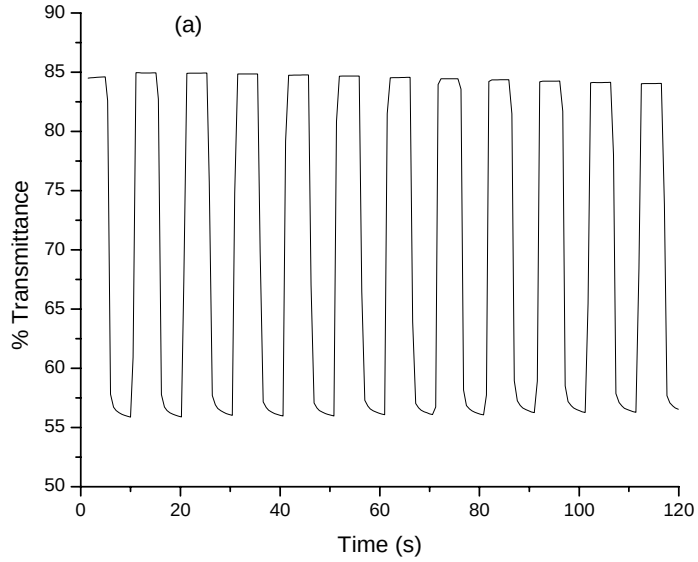

Figure 3.9 Electrochromic switching and optical absorbance change monitored at (a) 612 nm for P(DPOQ-co-BT)/PEDOT ECD between 0.0 V and +1.8 V

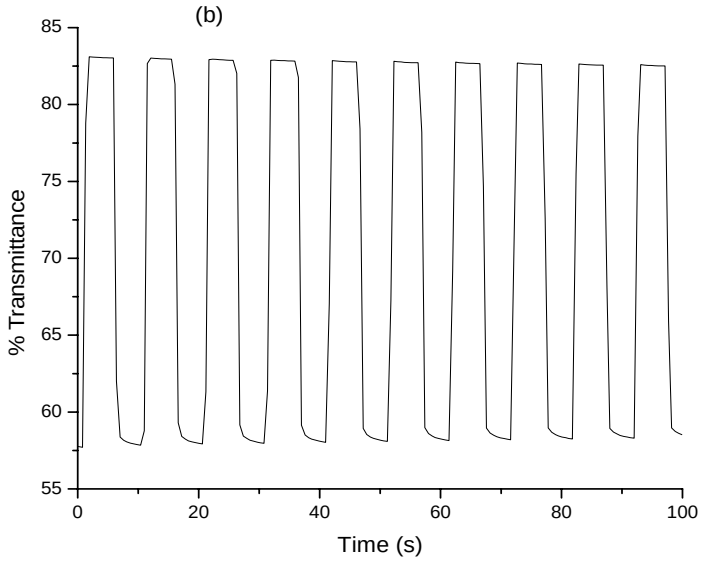

Figure 3.9 Electrochromic switching and optical absorbance change monitored at (b) 606 nm for P(DTTQ-co-BT)/PEDOT ECD between 0.0 V and +1.8 V

3.7.3 Stability of ECDs

Cyclic voltammetry method was used to evaluate the long-term stability of the devices. The potential was cycled between 0.0 and +1.8 V with 500 mV/s scan rate for P(DPOQ-co-BT)/PEDOT device (Figure 3.10 (a)). After 1000 cycles, 75% of its electroactivity was retained accompanied by unperturbed color change from orange to blue. For P(DTTQ-co-BT)/PEDOT device same procedure was applied and found that the device retains 72% of its electroactivity with a color change from red to blue (Figure 3.10 (b)). These results showed that both ECDs have good environmental and redox stability.

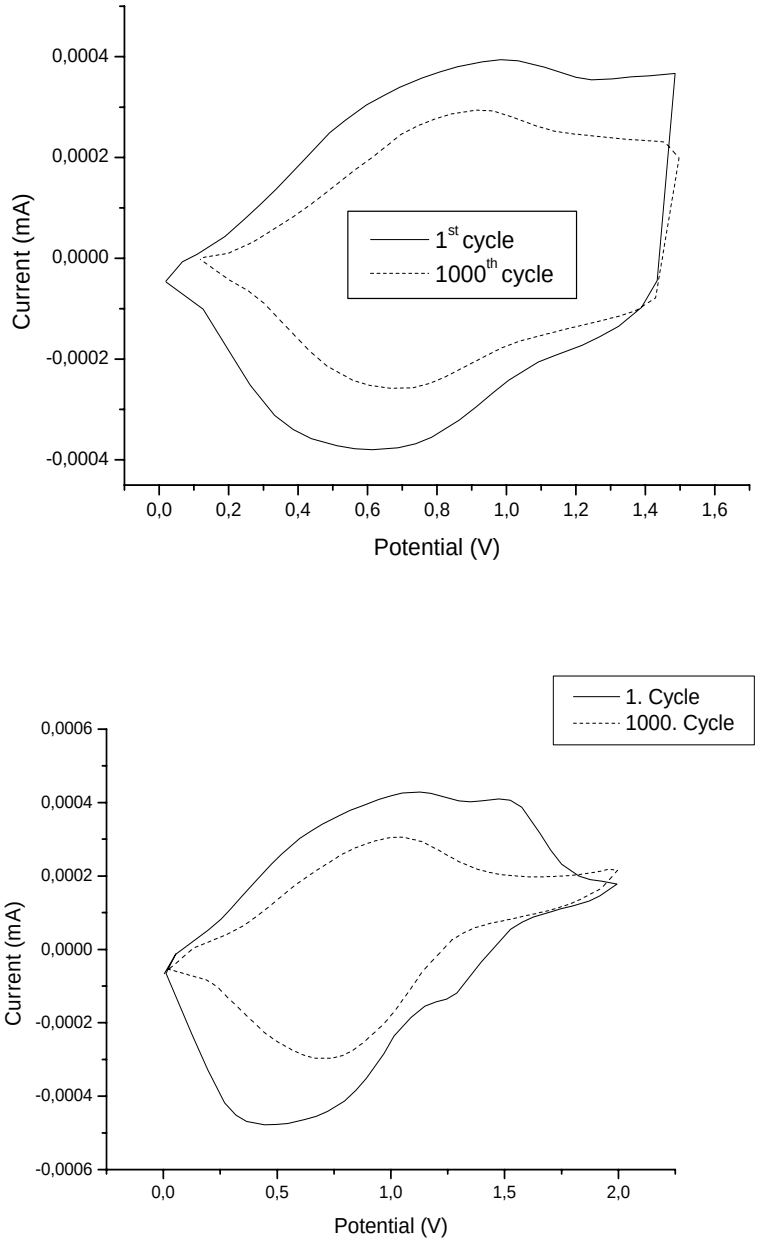

Figure 3.10 Stability test of (a) P(DPOQ-co-BT)/PEDOT ECD, (b) P(DTTQ-co-BT)/PEDOT ECD via cyclic voltammetry with a scan rate of 500 mV/s

3.7.4 Open Circuit Memory of ECDs

The open circuit memory of P(DPOQ-co-BT)/PEDOT device was tested at 0.0 V (orange colored state) and +1.8 V (blue colored state) at 455 nm and P(DTTQ-co-BT)/PEDOT device at 0.0 V (red colored state) and +1.8 V (blue colored state) at 485 nm. As seen in Figure 3.11 (a)-(b), P(DPOQ-co-BT)/PEDOT and P(DTTQ-co-BT)/PEDOT devices show quite good optical memories both in oxidized states (with only 1% transmittance change) and reduced states (with almost no transmittance change).

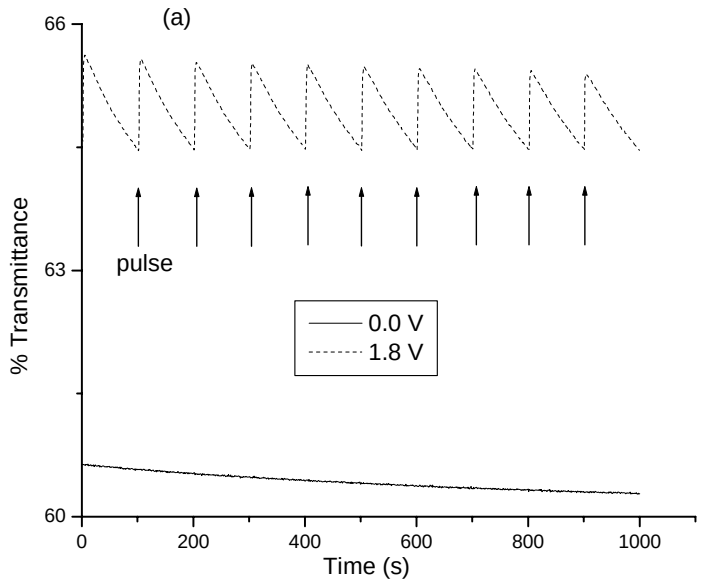

Figure 3.11 Open circuit memory of (a) P(DPOQ-co-BT)/PEDOT ECD monitored at 455 nm, 0.0 V and +1.8 V potentials were applied for one second for each 100 seconds time interval

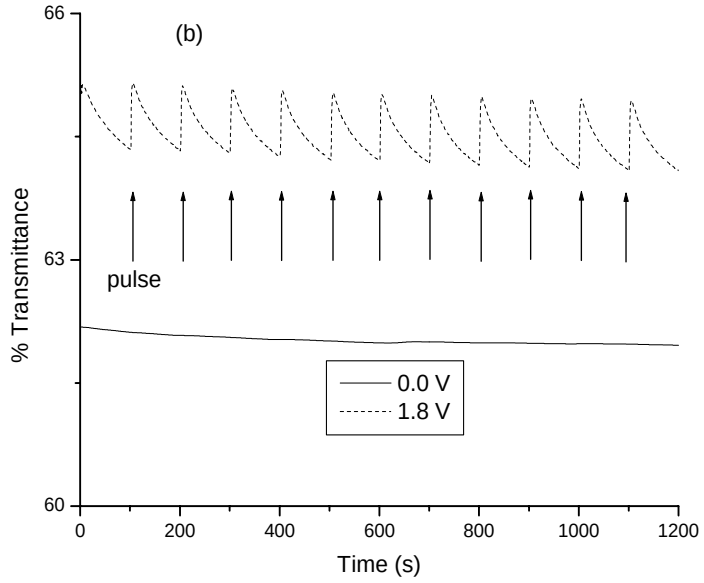

Figure 3.11 Open circuit memory of (b) P(DTTQ-co-BT)/PEDOT ECD monitored at 485 nm, 0.0 V and +1.8 V potentials were applied for one second for each 100 seconds time interval

3.7.5 Colorimetry Studies of ECDs

L*a*b values of the devices were measured at the fully oxidized and fully reduced states and the results are given in table 3.2. The extreme states and the colors at these states are given in figures 3.12 (a)-(b).

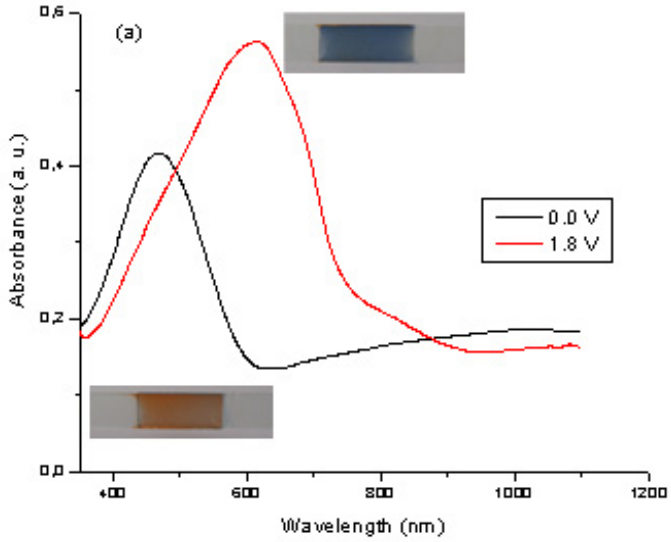

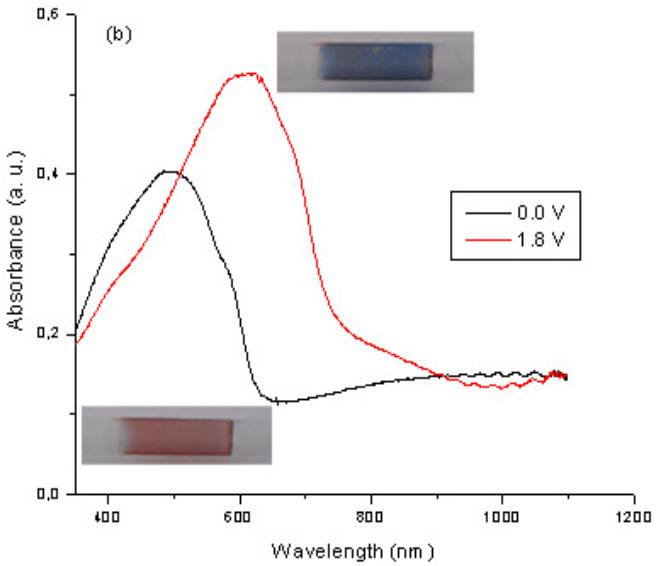

Figure 3.12 Extreme states of (a) P(DPOQ-co-BT)/PEDOT (b) P(DTTQ-co-BT)/PEDOT

Table 3.2 Electrochromic Properties of Devices

Material	**Color (ox)**	**Color (red)**	**L**	**a**	**b**
P(DPOQ-co-BT) /PEDOT	Blue	Orange	ox: 34 red: 17	ox: -3 red: 31	ox: -13 red: 23
P(DTTQ-co-BT) /PEDOT	Blue	Red	ox: 49 red: 35	ox: -1 red: 27	ox: -6 red: 11

ox: oxidized state

red: reduced state

CHAPTER IV

CONCLUSIONS

In this study, syntheses of two new monomers; 2-benzyl-5,12-dihydro-2*H*-pyrrolo[3',4':2,3][1,4]dioxocino[6,7-b]quinoxaline (DPOQ) and 5,12-dihydrothieno[3',4':2,3][1,4]dithiocino[6,7-b]quinoxaline (DTTQ) were successfully achieved. A conducting copolymer of DPOQ with bithiophene was synthesized potentiostatically in ACN/TBAFB (0.1 M) solvent-electrolyte couple and a conducting copolymer of DTTQ with bithiophene was achieved potentiodynamically in DCM/TBAFP (0.1 M) solvent-electrolyte couple. Cyclic voltammetry studies showed the electroactivity of DPOQ whereas electroactivity loss was observed for DTTQ. Copolymers; P(DPOQ-co-BT) and P(DTTQ-co-BT) revealed different redox behavior than that of both monomers and pure bithiophene. Copolymerization was also proved by FTIR and SEM studies. They were found to have reasonable conductivities. Spectroelectrochemical analyses revealed that the copolymers of DPOQ and DTTQ with bithiophene can be switched between their fully oxidized and fully reduced states with distinct color changes.

In the second part of the study, dual-type complementary colored polymer ECDs made up of P(DPOQ-co-BT)/PEDOT and P(DTTQ-co-BT)/PEDOT were constructed and their characteristics were examined. Devices exhibited reversible color change between the two states, reasonable stabilities, and good optical memories in their reduced state.

REFERENCES

1. D. Kumar, R. C. Sharma, *Eur. Polym. J.*, 34, 1053, 1998
2. M. Hatano, S. Kambara, S. Okamoto, *J. Polym. Sci.*, 51, S26, 1961
3. C. K. Chiang, C. R. Fincher, Jr., Y. W. Park, A. J. Heeger, and H. Shirakawa, E. J. Louis, S. C. Gau, A. G. Macdiarmid, *Phys. Rev. Letters*, 39, 1098, 1977
4. M. A. De Paoli, W. A. Gazotti, *J. Braz. Chem. Soc.*, 13, 410, 2002
5. A. J. Heeger, *J. Phys. Chem. B.*, 105, 36, 2001
6. D. L. Wise, G. E. Wnek, D. J. Trantolo, T. M. Cooper, J. D. Gresser, *Electrical and Optical Polymer Systems*, Marcel Dekker Inc., New York, 1998
7. A. F. Diaz, J. A. Logan, *J. Electroanal. Chem.*, 111, 111, 1980
8. G. Tourillon, F. Garnier, *J. Electroanal. Chem.*, 135, 173, 1982
9. A. Çırpan, S. Alkan, L. Toppare, I. Chianga, Y. Yagcı, *J. Mater. Sci.*, 37, 1767, 2002
10. H. L. Wang, L. Toppare, J. E. Fernandez, *Macromolecules*, 23, 1053, 1990
11. M. A. De Paoli, R. J. Waltman, A. F. Diaz, J. Bargon, *J. Polym. Sci. Poly. Chem. Ed.*, 23, 1687, 1985
12. W. A. Gazotti, G. Casalbore-Miceli, A. Geri and M. De Paoli, *Adv. Mater.*, 10, 60, 1998
13. G. Yu, A. J. Heeger, *Synth. Met.*, 85, 1183, 1997
14. J. H. Burroughes, D. D. C. Bradley, A. R. Brown, R. N. Marks, K. Mackay, R. H. Friend, P. L. Burns, A. B. Holmes, *Nature*, 347, 539, 1990
15. T. Matsunaga, H. Daifuku, T. Nakajima, T. Kavagoi, *Polym. Adv. Technol.*, 1, 33, 1990
16. B. Scrosati, *Polym. Int.*, 47, 50, 1998
17. N. Langsam, L. M. Robenson, *Polym. Eng. Sci.*, 29, 44, 1989
18. J. Gustafsson, O. Inganas, A. Anderson, *Synth. Met.*, 62, 17, 1994
19. M. De Paoli, S. Panero, S. Passerini, B. Scrosatti, *Adv. Mat.*, 2, 480, 1990
20. T. A. Skotheim, *Handbook of Conducting Polymers*, V2, Marcel Dekker, 1986

21. H. Shirakawa, E. J. Louis, A. G. MacDiarmid, C. K. Chiang, and A. J. Heeger, *Chem. Commun.*, 578, 1977
22. P. J. Nigrey, A. G. MacDiarmid, and A. J. Heeger, *Chem. Commun.*, 96, 594, 1979
23. A. J. Heeger, *Reviews of Modern Physics.*, 73, 681, 2001
24. N. F. Mort, E. A. Davis, *Electronic Processes in Non-Crystalline Materials*, Clarendon Press, Oxford, 1979
25. X. Li, Y. Jlao, S. Li, *Eur. Polym. J.*, 27, 1345, 1991
26. K. Pichler, D. A. Halliday, D. D. C. Bradley, P. L. Burn, R. H. Friend, A. B. Holmes, *J. Phys.: Condens. Matter*, 5, 7155, 1993
27. J. Roncali, *Chem. Rev.*, 92, 711, 1992
28. B. D. Malhotra, N. Kumar, S. Chandra, *Prog. Polym. Sci.*, 12, 179, 1986
29. A. F. Diaz, K. K. Kanazawa, in: J. S. Miller (Ed.), *Extended Linear Chain Compounds*, V3, Plenum Press, 1982
30. K. Gurunathan, A. Vadivel Murugan, R. Marimuthu, U. P. Mulik, D. P. Amalnerkar, *Mater. Chem. Phys.*, 61, 173, 1999
31. S. Hotta, S.D.D.V. Rughooputh, A. J. Heeger, *Synth. Met.*, 22, 79, 1987
32. J. Rodriguez, H. J. Grande, T. F. Otero, *Handbook of Organic Conductive Molecules and Polymers*, (Ed. H. S. Nalwa), John Wiley &Sons, 1997
33. S. Sadki, P. Schottland, N. Brodie, G. Sabouraud, *Chem. Soc. Rev.*, 29, 283, 2000
34. N. M. Rowley, R. J. Mortimer, *Sci. Prog.*, 85, 243, 2002
35. T. Bange, T. Gambke, *Adv. Mat.*, 2, 10, 1990
36. B. Scrosati, *Applications of Electroactive Polymers*, Chapmann&Hall, London, 1993
37. P. M. S. Monk, R. J. Mortimer, D. R. Rosseinsky, *Electrochromism: Fundamentals and Applications*, VCH, Weinheim, 1995
38. M. Green, *Chem. Ind.*, 17, 641, 1996
39. R. J. Mortimer, *Chem. Soc. Rev.*, 26, 147, 1997
40. P. Camurlu, A. Cirpan, L. Toppare, *J. Electroanal. Chem.*, 572, 61, 2004

41. B. C. Thompson, P. Schottland, Z. Kyukwan and J. R. Reynolds, *Chem. Mater.*,12, 1563, 2000
42. S. A. Sapp, G. A. Sotzing and J. R. Reynolds, *Chem. Mater.*, 10, 2101, 1998
43. E. M. Girotto, M. De Paoli, *J. Braz Chem. Soc.*, 10, 394, 1999
44. P. R. Somani, S. Radhakrishnan, *Mater. Chem. Phys.*, 77, 117, 2002
45. (a) F. Wudl, M. Kobayashi, A.J. Heeger, *J. Org. Chem*., 49, 3382, 1984, (b) T. C. Chung, J. H. Kaufman, A. J. Heeger, F. Wudl, *Phys. Rev. B.*, 30, 702, 1984, (c) M. Kobayashi, N. Colaneri, M. Boysel, F. Wudl, A. J. Heeger, *J. Chem. Phys.*, 82, 5717, 1985, (d) H. Yashima, M. Kobayashi, K. B. Lee, D. Chung, A. J. Heeger, F. Wudl, *J.Electrochem. Soc.*, 134, 46, 1987
46. (a) G. Heywang, F. Jonas, *Adv. Mat.*, 4, 116, 1992 (c) M. Dietrich, J. Heinze, G. Heywang, F. Jonas, *Electroanal. Chem.*, 369, 87, 1994
47. A. Cirpan, A. A. Argun, C. R. G. Grenier, B. D. Reeves and J. R. Reynolds, *J. Mater. Chem.*, 13, 2422, 2003
48. K. Kham, S. Sadki, C. Chevrot, *Synth. Met.*, 145, 135, 2004
49. S. Roquet, P. Leriche, I. Perepichka, B. Jousselme, E. Levillain, P. Frere, J. Roncali, *J. Mater. Chem.*, 14, 1396, 2004

PUBLICATION

S. Beyazyildirim, P. Camurlu, D. Yilmaz, M. Gullu, L. Toppare “Synthesis and electrochromic properties of conducting copolymers of dioxocino- and dithiocino-quinoxalines with bithiophene” (Submitted 2004)